CHALMERS

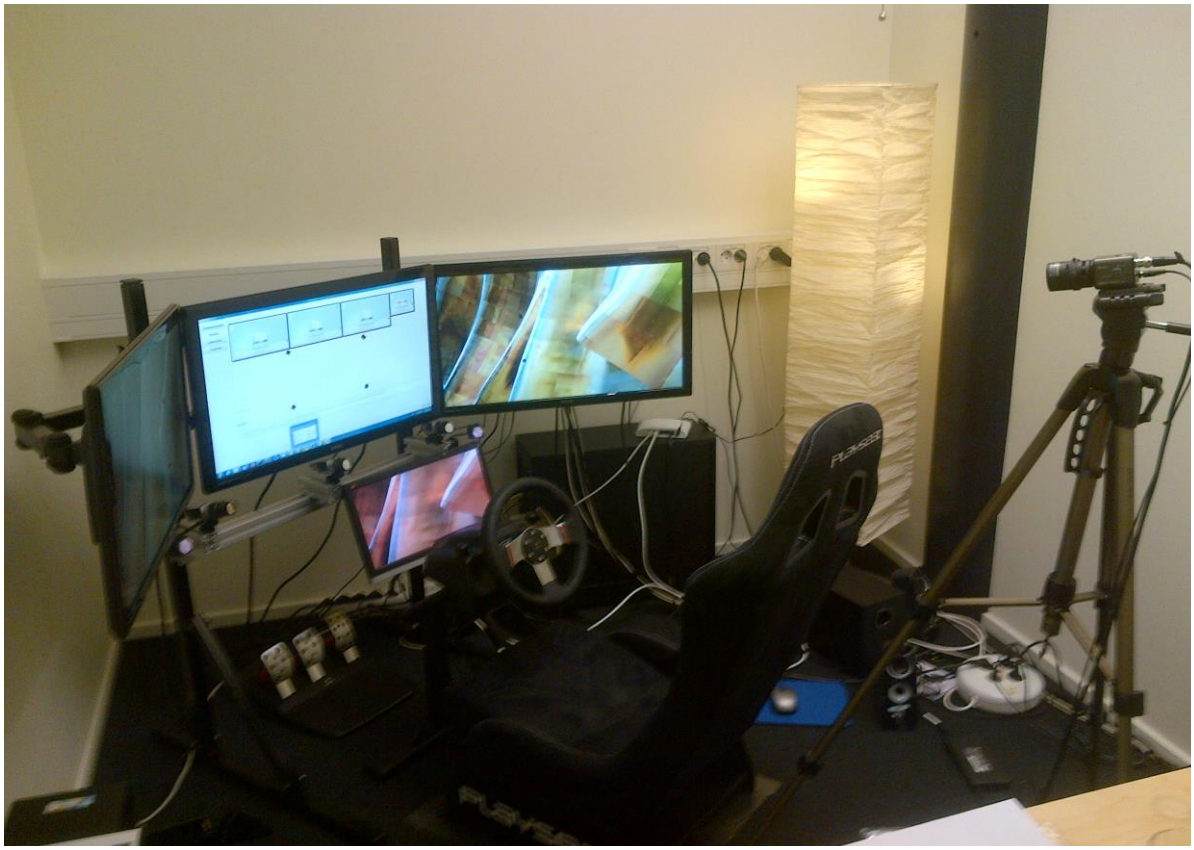

Desktop Driving Simulator with Modular Vehicle Model and Scenario Specification

Master's Thesis, Master's Programme Automotive Engineering

ARPIT KARSOLIA

Department of Applied Mechanics
Division of Vehicle Engineering & Autonomous Systems
Vehicle Dynamics group
CHALMERS UNIVERSITY OF TECHNOLOGY
Göteborg, Sweden 2014
Master's thesis 2014:06

MASTER'S THESIS

Desktop Driving Simulator with Modular Vehicle Model and Scenario Specification

ARPIT KARSOLIA

Department of Applied Mechanics
Division of Vehicle Engineering & Autonomous Systems
Vehicle Dynamics group

CHALMERS UNIVERSITY OF TECHNOLOGY
Göteborg, Sweden

Desktop Driving Simulator with Modular Vehicle Model and Scenario Specification

ARPIT KARSOLIA

Master's Thesis 2014:06
ISSN 1652-8557
Department of Applied Mechanics
Division of Vehicle Engineering & Autonomous Systems
Vehicle Dynamics group

Chalmers University of Technology
SE-412 96 Göteborg
Sweden
Telephone: + 46 (0)31-772 1000

Cover:
3-Screen Desktop Simulator as used in simulator trials with 4 camera eye tracking system.

Chalmers reproservice/Department of Applied Mechanics
Göteborg, Sweden 2014

Desktop Driving Simulator with Modular Vehicle Model and Scenario Specification

Master's Thesis

ARPIT KARSOLIA

Department of Applied Mechanics

Division of Vehicle Engineering & Autonomous Systems

Vehicle Dynamics group
Vehicle Dynamics
Chalmers University of Technology

ABSTRACT

Driving Simulators are one of the key tools to simulate and verify, interactions between vehicle & driver in a realistic as well as conditioned traffic environment. Real vehicle testing and pure simulation (using a driver model) are two alternative tools of collecting such information. Relevant data from real vehicle testing requires a high degree of repetition, man-power and is time-consuming, not to mention expensive. Advanced driver simulators are present in Sweden which provide, very realistic driver experience and perception. They simulate, very accurately, a real-time scenario in a holistic environment. But, in the modern world, vehicle & traffic situations have become so complex that the application and usefulness of driver simulators has moved beyond its usual definition. Thus, every experiment goes through an intricate, time consuming and thus expensive process of experimental design & development. The solution proposed in this thesis is to use a driving simulator which is portable and can simulate an experiment/scenario at an office level before moving to advanced simulators or real testing. The Desktop driving simulator would provide a platform to test a potential idea at a lesser scale and establish its functionality. This thesis will also study the modularity of the vehicle model for parameterization and simulate common vehicle manoeuvres to investigate model accuracy. However, results obtained will not be at par with analysis on advanced simulators, especially regarding driver perception and response but may provide an indication towards its behaviour and relevance.

Key words: driving simulator, scenario, testing, driver perception, vehicle model.

Contents

ACRONYMS II

1 INTRODUCTION 3

1.1 Thesis Description 4
1.1.1 Goals & Deliverables 4
1.1.2 Research Questions 5
1.1.3 Intended User 5
1.1.4 Test Vehicles Description – Ambulances 6
1.1.5 Scenario III 6
1.1.6 Thesis Limitations 7

1.2 Theory of Vehicle Dynamics 8
1.2.1 Position of Centre of Mass[4] 8
1.2.2 Height of Centre of Mass[4] 8
1.2.3 Vehicle at Braking & Driving[3] 9
1.2.4 Tire Slip and Vehicle Behaviour 9
1.2.5 The Magic Formula Tire Model[3] 10

2 SIMULATOR DESIGN 11

2.1 Components – HW & SW 11

2.2 Visual Display Flowchart 11

2.3 Vehicle Model 12
2.3.1 Model Communication 12
2.3.2 Model Structure 13
2.3.3 Model Blocks 14
2.3.4 Offline & Online model structure 24
2.3.5 Electronic Stability Control system 26
2.3.6 Parameterised Models – Ambulances 28

3 SIMULATOR SCENARIOS 30

3.1 Obstacle Avoidance 31

3.2 Simulation Tests 32
3.2.1 Straight Line Braking ISO 21994 32
3.2.2 Sine wave with Dwell (SWD) TP-126-03 33
3.2.3 Double Lane Change – ISO 3888-1 34

4 SIMULATION RESULTS 36

4.1 Obstacle Avoidance 36

4.2 Straight Line Braking 36
4.2.1 Volvo S40 2L (2007) 38
4.2.2 Mercedes Sprinter (2013) 41

4.3 Sine with Dwell Test - Offline 44

4.3.1 Mercedes VitoXL (2013) 45
4.4 DLC manoeuvre – Online 49

5 CONCLUSIONS & FUTURE WORK 52
5.1 Conclusions 52
5.2 Future Work 53

6 REFERENCES 54

APPENDIX A – VEHICLE MODEL I/O 56

APPENDIX B – SWD PLOTS VOLVO S40 59

APPENDIX C – DLC PLOTS MERCEDES VITOXL 62

APPENDIX D - VOCABULARY (ISO - 8855)[23] 64

APPENDIX E – VEHICLE PARAMETERS 65

APPENDIX F – LOGGED VARIABLES 70

Preface

In this thesis, offline and online testing of the vehicle model with 2 different sets of ambulance vehicle data were carried out using Matlab/Simulink & software provided by VTI. The tests were carried out from May 2014 to August 2014. This thesis is part of a research project called ASTAZero SIM based on the ASTAZero Track, in Borås (project funded by Vinnova, reference Diarienummer 2013-04715). The thesis was carried out at the Department of Applied Mechanics, Division of Vehicle Engineering & Autonomous systems, Chalmers University of Technology, Sweden. The ASTAZero SIM project is a joint enterprise of Chalmers University with VTI and SP.

A part of this thesis has been carried out with Matteo Santoro as a fellow thesis teammate and Prof. Bengt Jacobson & Prof. Jonas Sjöberg as supervisors. All simulations were carried out with the simulator equipment at Chalmers University of Technology. I would like to thank Eleni Kalpaxidou, Jonas Andersson Hultgren, Sogol Kharrazi and Ingvar Näsman from VTI, Martin Skoglund, Niklas Adolfsson & Erik Torstensson from SP, and Anders Karlsson from Chalmers for their co-operation and support in dealing with the simulation software and hardware. A special mention to Artem Kusachov from VTI/Chalmers for taking the time to review important sections of this report and conveying suggestions to improve its overall credibility.

Finally, I would like to thank Matteo Santoro & my supervisors for helping me through this thesis and in achieving satisfactory results.

Göteborg November 2014

Arpit Karsolia

Notations

a	Longitudinal Position w.r.t Centre of Gravity, C.G.
$A0$	Frontal Area
a_y	Lateral Acceleration
b	Lateral Position w.r.t C.G.
Cax	Coefficient of Air Drag
$Cdamp$	Damping Coefficient at wheel position, per side (Front, Rear)
f_r	Rolling Resistance coefficient
$F_{x\ tire}$	Longitudinal Tire Force
$F_{y\ tire}$	Lateral Tire Force (LF, RF, LR, RR)
F_z	Vertical Force
GR_{tot}	Total Gear ratio
h_{cg}	Height of C.G
hr	Roll Centre Height
hsr	Height of C.G above Roll Axle
hus	Height of unsprung mass centre
I_{drv}	Driveshaft moment of Inertia
I_{eng}	Engine moment of Inertia
I_r	Moment of Inertia around Roll axle
I_w	Wheel rotational moment of Inertia
I_y	Pitch Moment of Inertia around C.G
I_z	Moment of Inertia about Z-axis
$Karb$	Anti-Bar Roll Stiffness (Front, Rear)
$Kspr$	Spring Coefficient at wheel position, per side (Front, Rear)
lf	Front Axle longitudinal distance from C.G.
lr	Rear Axle longitudinal distance from C.G.
m	Vehicle Mass
ms	Total Sprung Mass
mus	Total Unsprung Mass(Axle)
mus	Unsprung Mass per side (Front, Rear)
M_z	Tire Aligning Torque
R_w	Wheel Radius

SG_ratio	Steering Gear Ratio
T_{q_drv}	Driveline Torque
T_{qbrk}	Brake Torque
tw_f	Track width – Front
tw_r	Track width – Rear
$V_{x\ slip}$	Minimum velocity for Longitudinal Slip Calculation
V_x	Longitudinal Vehicle Velocity
V_y	Lateral vehicle velocity
X	Vehicle position in global coordinates (X-axis)
Y	Vehicle position in global coordinates (Y-axis)
Zcg	Vertical Position of C.G.
Z_w	Vertical Position of road wheel
γ	Wheel Camber angle
δ	Steering Angle
θ	Pitch Angle
κ	Longitudinal Slip
ρ	Density of Air
Φ	Roll Angle
Ψ	Yaw angle
Ψ_{0_static}	Static Toe Angle
ω_{whl}	Wheel velocity

Acronyms

ABS	*Anti-Lock Braking System*
ESC	*Electronic Stability Control*
DOF	*Degree of Freedom*
ASTAZero	*Active Safety Test Area Zero*
HW	*Hardware*
SW	*Software*
UDP	*User Datagram Protocol*
LAN	*Local Area Connection*
LF	*Left Front*
RF	*Right Front*
LR	*Left Rear*
RR	*Right Rear*
FWD	*Front Wheel Drive*
RWD	*Rear Wheel Drive*
AWD	*All Wheel Drive*
MF	*Magic Formula*
CG	*Centre of Gravity*
EBD	*Electronic Brake Force Distribution*
DSTC	*Dynamic Stability & Traction Control*
EBA	*Electronic Brake Assist*
BAS	*Brake Assist System*
ASR	*Acceleration Skid Control*
SWD	*Sine with Dwell*
DLC	*Double Lane Change*
CCW	*Counter Clockwise*

List of Figures

Figure 1.1 *Driving Simulator Hierarchy*

Figure 1.2 *ASTAZero Track Environment*

Figure 1.3 *Scenario III*

Figure 1.4 *Experimental Determination of longitudinal position of centre of mass*

Figure 1.5 *Automobile subjected to longitudinal forces & subsequent load transfer*

Figure 1.6 *Curve produced by the original sine version of the Magic Formula*

Figure 2.1 *Chalmers Simulator structure*

Figure 2.2 *Flowchart of Visual Display*

Figure 2.3 *Communication – External Vehicle Model*

Figure 2.4 *Model Overview*

Figure 2.5 *Steering Torque structure*

Figure 2.6 *Brake block*

Figure 2.7 *Magic Formula 5.2 subsystem*

Figure 2.8 *Function block – Magic Formula*

Figure 2.9 *Chassis block*

Figure 2.10 *Road subsystem*

Figure 2.11 *ESC Overview*

Figure 2.12 *ESC Structure*

Figure 3.1 *Simulation Flowchart*

Figure 3.2 *Obstacle Avoidance*

Figure 3.3 *Straight Line Braking*

Figure 3.4 *Offline Driver Input - Straight Line Braking (S40)*

Figure 3.5 *Offline Driver Input Test 2 – Sine wave with Dwell (S40)*

Figure 3.6 *Placing of cones for DLC track*

Figure 4.1 Longitudinal Force Coefficient as a function of longitudinal slip

Figure 4.2 Vehicle Speed (km/h) vs Time(s) (S40)

Figure 4.3 X-position (m) vs Time(s) (S40)

Figure 4.4 Vehicle Velocity (m/s) & Wheel Velocity (m/s) vs Time(s) – LF & RR (S40)

Figure 4.5 Vehicle Velocity (m/s) & Wheel Velocity (m/s) vs Time(s) – LF & RR (ABS) (Sprinter)

Figure 4.6 Tire Longitudinal Slip vs Time(s) (ABS) (Sprinter)

Figure 4.7 Longitudinal Tire Force (N) vs Longitudinal Slip – LF & RR (ABS) (Sprinter)

Figure 4.8 Steering Input & Path Plots – Volvo S40 with ESC

Figure 4.9 Vehicle Behaviour for different paths

Figure 4.10 Path Plot – Mercedes VitoXL with/without ESC

Figure 4.11 Brake Torque (Nm) vs Time (s) – Mercedes VitoXL with ESC

Figure 4.12 Lateral slip angle (rad) vs Time (s) – LF, RF, LR, RR Tires (VitoXL)

Figure 4.13 Vehicle body slip angle (deg) vs Time (s) – with/without ESC (VitoXL)

Figure 4.14 DLC path and key positions

Figure 4.15 DLC path with/without ESC (VitoXL)

Figure 4.16 Steering Wheel Angle & X-position vs Time (VitoXL)

List of Tables

Table 2.1 *Parameters for wheels*

Table 2.2 *Output signals from driver to model*

Table 2.3 *Signals from road to model*

Table 2.4 *Scaled variables*

Table 3.1 *Vehicle & Simulation Type for given manoeuvre*

Table 3.2 *SWD settings*

Table 3.3 *Dimensions of DLC track*

Table 4.1 *Vehicle Specs*

Table 4.2 *ABS Simulation Settings (S40)*

Table 4.3 *Maximum Brake Torque per axle (S40)*

Table 4.4 *Simulation Stopping Distance & Duration (S40)*

Table 4.5 *ABS Simulation Settings (Sprinter)*

Table 4.6 *Maximum Brake Torque per axle (Sprinter)*

Table 4.7 *Simulation Stopping Distance & Duration – Sprinter*

Table 4.8 *ESC settings for Mercedes VitoXL*

Table 4.9 *Steer and Path Points for SWD steer – Mercedes VitoXL with ESC*

Coordinate System

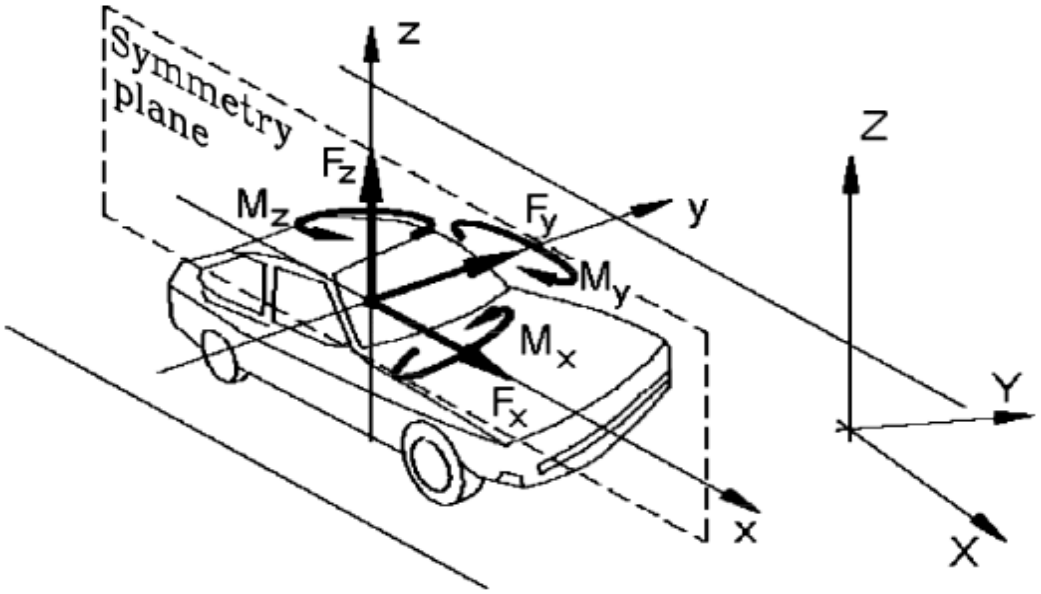

Figure – Vehicle Body Coordinate System[4]

OVE = Own Vehicle (simulator vehicle)

OVE origo = centre point of front wheel axis

For the online simulations, three coordinate systems were used –

1. Body Fixed System, right handed Cartesian DIN – system
    - X is Forward
    - Y is Left
    - Z is Upward
    - CCW is positive angle

2. Track System, (non-linear road following) right handed system
    - s is position of OVE origo along chord line from the beginning of the road calculated in XY – plane (no elevation taken into account)
    - r is lateral position OVE origin with respect to road centre coordinate line
    - h is height above road surface
    - yaw is CCW positive angle with respect to centre coordinate line tangent

3. Inertial System, world global right-handed Cartesian system
    - X is east
    - Y is north
    - Z is up
    - Heading is CCW positive angle, with respect to east direction.

1 Introduction

Driving Simulators provide an essential link between an engineer's idea for development and actual testing of the idea itself. The definition of a driving simulator can range from a basic computer model simulating a particular dynamic element of vehicle behaviour to a multiple DOF, high fidelity structure, accurately simulating real time behaviour. On the basis of simulation mode, a driving simulator can also be defined as an offline or an online mode.

An offline mode would generally be pure simulation (non-real time) & represents simulations carried out on a PC with a vehicle model designed on platforms such as Matlab, Simulink, Dymola, etc., with different vehicle parameters fed as inputs. The vehicle model would range from a quarter car representation to a double track model. The model inputs can be pre-defined signals written in code or built signal shapes. Most commonly discussed vehicle model type is the Bicycle (single track) model. It generally caters for linear vehicle behaviour with specific assumptions. Also, to model certain active safety systems like ESC, ABS, etc., a bicycle model is used as a reference model in the design. One of the limitations of offline simulations is that it doesn't have a graphical interface or representation to visualize simulations as they are carried out. With reference to Figure 1.1, a scroll model is another type of vehicle model. It may or may not be real time. A scroll model allows you to rapidly change the model inputs using a scroll bar which can be used for pedals & steering wheel inputs. This provides more control during a simulation.

An online mode refers to a synchronisation of a vehicle model with a graphical interface/representation while running in real time. The structure would consist of a hardware element which would be the source of input for the simulation software. Depending on the level of complexity, the online mode would cover a range of simulators from an office level desktop simulator to a multiple DOF motion simulator.

This thesis refers to the office-level desktop simulator which provides a simpler & portable platform for online simulations with varying levels of realism. Figure 1.1 represents a hierarchy of common types of simulators which have been encountered during the course of this thesis. They have been judged on the basis of model flexibility/physical portability & levels of realism. For this thesis, flexibility of a model represents its ability to switch to different vehicles rapidly without requiring complex model tuning. However, realism would represent how close a simulator is to representing real vehicle behaviour. On this scale then, the most flexible/portable type would be an offline simulation setup and the most realistic would be a real test vehicle. However, this plot is used for representation purposes based on understanding during the course of this thesis and may not be accurate globally. Also, as simulators are judged on the basis of driver's perception of his surroundings and 'feel', the position of the different simulators in Figure 1.1 may vary comprehensively.

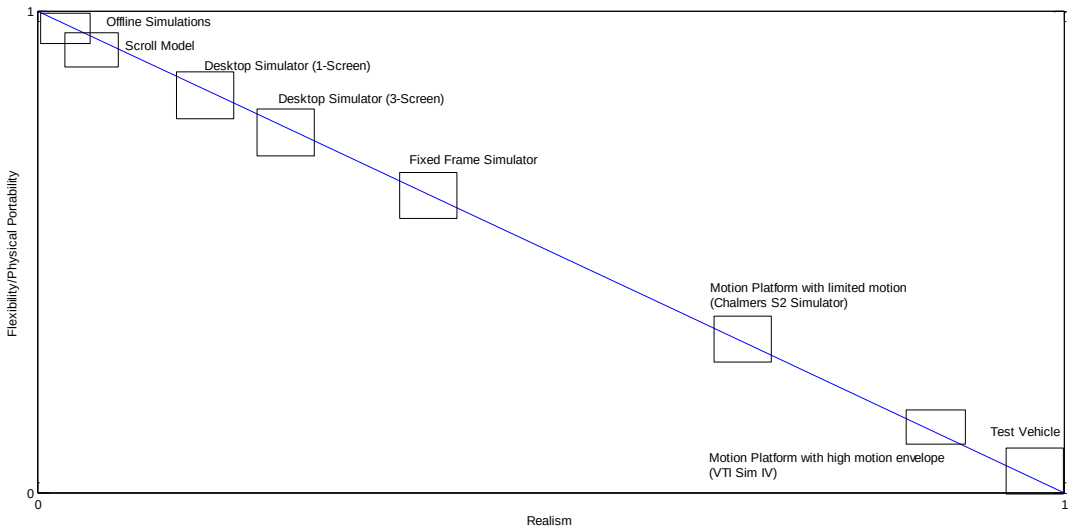

Figure 1.1 Driving Simulator hierarchy

The Chalmers Desktop Simulator is presented under the ASTAZero project based on the test track in Borås. The ASTAZero project represents a test environment for technological advancements on road & traffic safety systems. One of the first projects involves enhancement of safety protocols for ambulance drivers by simulating dangerous road situations in a conditioned test environment. This thesis deals with one of the driving scenarios suggested by Region Västra Götaland (VGR) and aims to simulate this scenario while using the standard ambulance vehicles.

1.1 Thesis Description

The Chalmers Desktop Simulator comprises of a hardware setup supported by a vehicle model designed in Simulink & a 'graphical representation' designed in Qt Creator. A comprehensive evaluation of the vehicle model while establishing its modularity with offline and online manoeuvres is described in this thesis along with an advanced case study on a particular scenario suggested by Region Västra Götaland (VGR). The offline and online manoeuvres are chosen such that they indicate possible driver behaviour during the advanced scenario.

This thesis also intends to provide a parameterised vehicle model having ESC & ABS functionalities with moderate levels of tuning conducted to incorporate the different ambulance vehicles to be used for testing.

This thesis should be able to provide a platform for further development of the desktop simulator at Chalmers and contribute towards the ASTAZero project in a minor capacity.

1.1.1 Goals & Deliverables

1. Establish modularity of vehicle model
2. Verification of the vehicle model by displaying flexibility of model equations & parameters for parameterization of multiple vehicles.

a. Offline Simulations
    - Straight line Braking Test (also Online)
    - Sine With Dwell steer

b. Online Simulations
    - Simple Case - Double Lane Change (ISO 3881)

3. Establish ESC and ABS functionality for the vehicle model and tune parameters accordingly.
4. Case study of 'Scenario III' (advanced) to describe/show vehicle behaviour.

1.1.2 Research Questions

1. Do ABS/ESC subsystems display functionality when integrated into vehicle model and in simulator? Do they activate/function for online simulations? If yes, how accurate are the results?

2. (a) Is it possible to parameterize the vehicle model with a few parameters and still represent a decent behaviour when changing between different vehicle types?

   (b) As vehicle model is parameterized to multiple vehicles (Sedan passenger car and various weight ambulances), do ABS/ESC subsystems survive parameterization?

3. Is simulator realistic enough to show/measure difference with/without ABS/ESC systems?

1.1.3 Intended User

As stated earlier, the Desktop simulator is intended for usage at an office-level. The targeted user of this simulator would be an engineer working on the simulation team for a particular project, as the simulator would be able to provide him/her with sufficient simulation data to further investigate the potential idea before moving toward higher fidelity simulators. However, results are not intended to be at par with higher fidelity simulators.

For the ASTAZero project, this simulator is seen as a training tool to get potential drivers familiar with the ASTAZero environment, the scenarios and provide them adequate training before moving to the track.

1.1.4 Test Vehicles Description – Ambulances

The external vehicle model is parameterized to standard ambulance vehicles which are utilised by Region Västra Götaland (VGR) in Sweden currently. The ambulances are the Mercedes VitoXL(AWD) and Sprinter (RWD) with low roof and high roof options. Vehicle specifications can be found in Appendix. A base vehicle (S40) was also used to judge the functionality of the ABS & ESC systems.

However, during the course of this thesis, a complete set of parameter values, as needed by the vehicle model, could not be accurately compiled. Due to this, a method of scaling parameter values from the base vehicle was implemented to complete the list for the ambulances.

1.1.5 Scenario III

The three preliminary scenarios suggested by VGR are to be tested on the ASTAZero Track as shown in Figure 1.2.

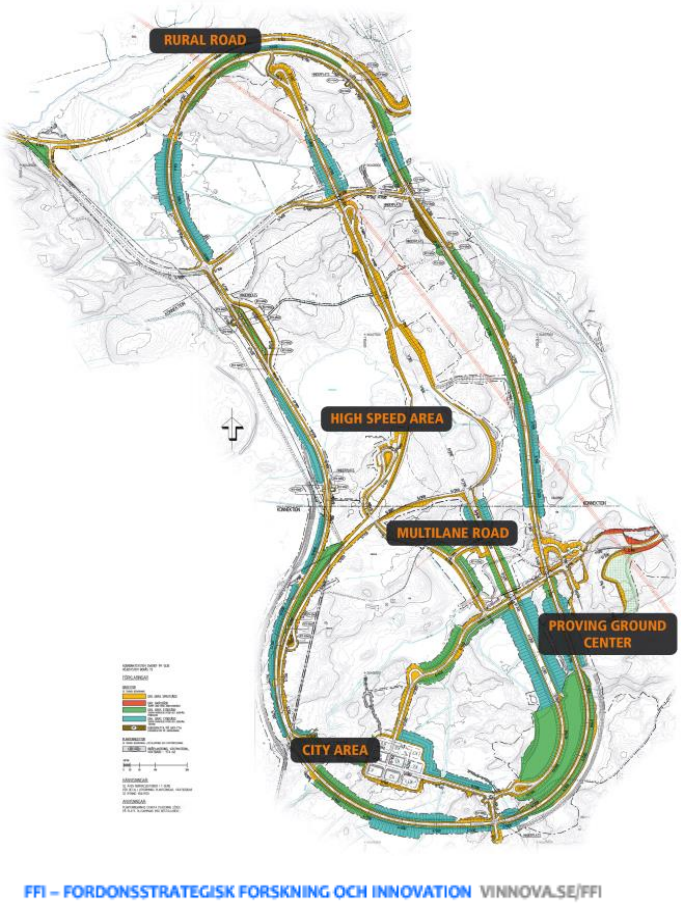

Figure 1.2[8] ASTAZero Track Environment

One of the three scenarios suggested, is focused on, in this thesis. Scenario III uses the rural road environment on the ASTAZero track. As the track consists of a loop, the scenario will be performed depending on the driver lap.

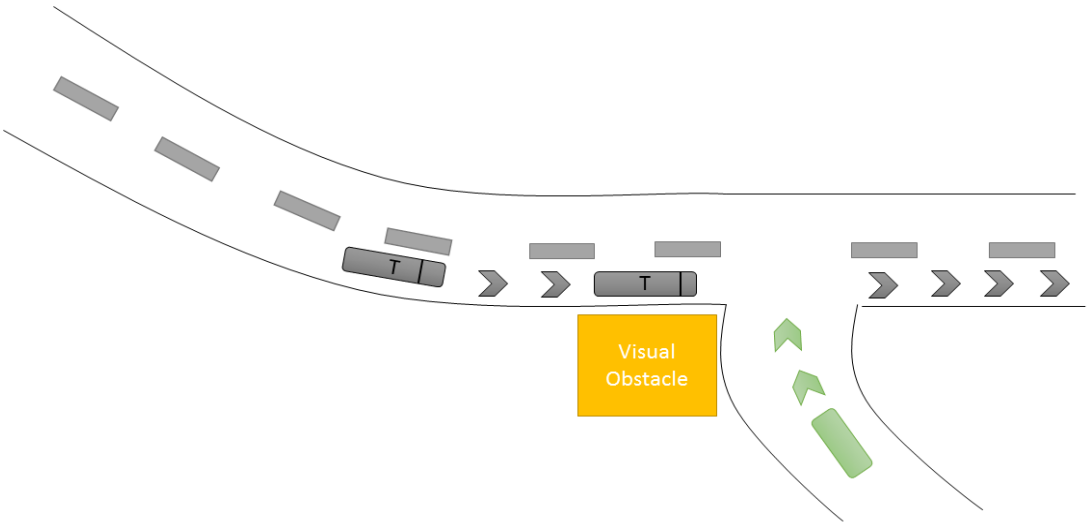

Figure 1.3 Scenario III

Figure 1.3 illustrates the scenario III and is basically a visual obstruction scenario. The test vehicle approaches an intersection or a crossing but the driver's vision is obstructed so it is unable to see the 'balloon' car approaching the crossing. As the balloon car joins the road, the test vehicle employs evasive driving behaviour which may either be full brake or a single/double lane change. In this thesis, the original scenario is modified and instead of a balloon car, position triggered cones are utilised to simulate the same response. The modified scenario will elaborated upon in Section 3.1.

1.1.6 Thesis Limitations

1. As the vehicle model demands more vehicle parameters than publically available, it hinders the accuracy of the simulation results.

2. For this simulator, flexibility and physical portability is an integral part of the purpose. This implies that it should be a self-sufficient package. The usage of an Ethernet-specific external PC for real time simulation is considered as an accepted exception from this intention.

3. Scenario modularity was restricted to 3 different environments – rural road, highway and country-side. Modularity couldn't be explored for roads with different friction conditions.

4. In terms of visual display, the driver does not see the width of the car and does not experience (visually) pitch and roll movements.

5. As the project is still ongoing, the thesis does not intend to document the vehicle model and scenarios model entirely as modular parts of the overall software architecture. Instead, the thesis refers to future documentation from overall ASTAZero SIM project

1.2 Theory of Vehicle Dynamics

1.2.1 Position of Centre of Mass[4]

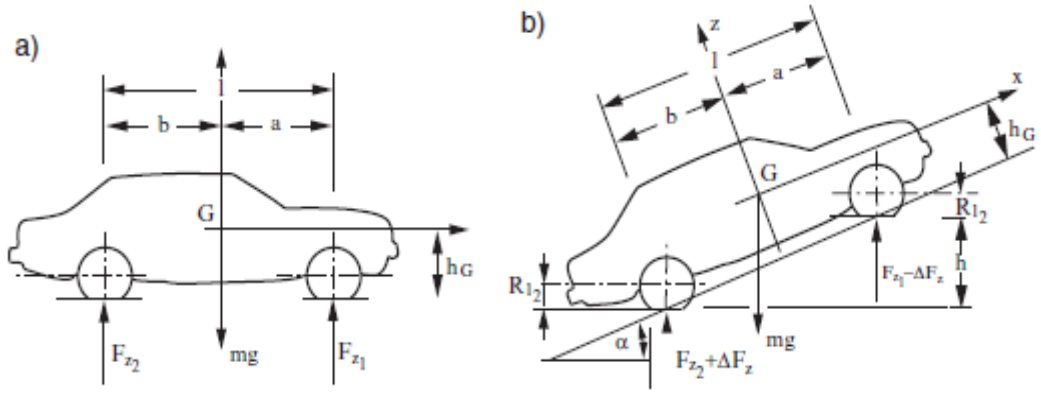

Figure 1.4 Experimental Determination of longitudinal position of centre of mass[4]

Equations to determine longitudinal position using equilibrium equations, with reference to Figure 1.4(a) -

$$F_{z1} + F_{z2} = mg \tag{1.1}$$

$$lF_{z1} = b * m * g \tag{1.2}$$

$$a = l\frac{F_{z2}}{F_{z1} + F_{z2}} \tag{1.3}$$

$$b = l\frac{F_{z1}}{F_{z1} + F_{z2}} \tag{1.4}$$

1.2.2 Height of Centre of Mass[4]

With reference to Figure 1.4(b), the front axle is set on a platform with height h with respect to the platform on which the rear axle is located. If h_G is greater than radius under load of the wheels, the force F_{z1}', measured at the front axle is much smaller than that measured on level road, then –

$$F_{z1}' = F_{z1} - \Delta F_z \tag{1.5}$$

$$F_{z2}' = F_{z2} + \Delta F_z \tag{1.6}$$

So, the equilibrium equation for rotations about the centre of the front axle is –

$$mg[a\cos(\alpha) + (h_G - R_{l1})\sin(\alpha)] = (F_{z2} + \Delta F_z)[l\cos(\alpha) + (R_{l2} - R_{l1})\sin(\alpha)] \tag{1.7}$$

This implies, the centre of mass –

$$h_G = \frac{F_{z2} + \Delta F_z}{mg}\left[\frac{l}{\tan(\alpha)} + R_{l2} - R_{l1}\right] - \frac{a}{\tan(\alpha)} + R_{l1} \tag{1.8}$$

1.2.3 Vehicle at Braking & Driving[3]

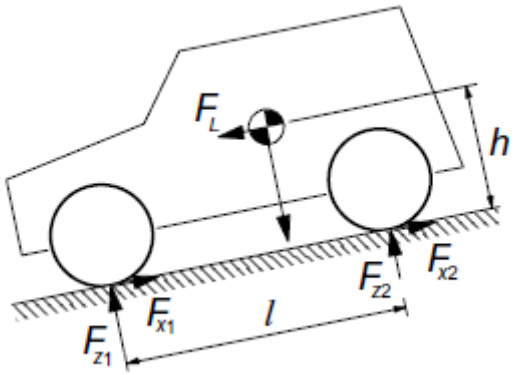

Figure 1.5 Automobile subjected to longitudinal forces & subsequent load transfer[3]

As shown in Figure 1.5, when a vehicle is subjected to longitudinal forces from braking, to compensate for wind drag or down or upward slopes, longitudinal load transfer occurs.

Change in tire normal loads causes change in cornering stiffness's & the peak side forces on the axle's change. This effects the handling behaviour of the vehicle with the increase or decrease of understeer gradient.

Braking forces also give rise to a state of combined slip and hence effecting lateral forces. At hard braking, tending the wheels to lock, stability and steer ability deteriorates severely.

1.2.4 Tire Slip and Vehicle Behaviour

The directional behaviour of a vehicle is deeply influenced by longitudinal forces between tires and road. Longitudinal force causes a reduction in cornering stiffness, hence, when applied to the front axle, the vehicle becomes more understeer or less understeer. Whereas, when applied in the rear, it causes the opposite effect[4].

For a linearized model[4],

$$C_i = C_{0_i}\sqrt{1-\left(\frac{F_{x_i}}{\mu_p F_{z_i}}\right)^2} \tag{1.9}$$

A larger ratio F_x / F_z at the rear wheels makes the vehicle more oversteer and readily introduces a critical speed[4]. As limiting conditions are reached, a spinout is expected unless the driver reduces the longitudinal forces and counter steers[4]. To avoid this, anti-spin and anti-lock devices are essential[4]. Poor road conditions (road friction) also influence the F_x / F_z ratio hence contributing to vehicle behaviour.

A change in tire lateral slip also effects the tire cornering stiffness's, thereby influencing tire forces (lateral & longitudinal) and hence vehicle stability.

Magic formula is an example displaying the influence of tire slip on tire forces.

1.2.5 The Magic Formula Tire Model[3]

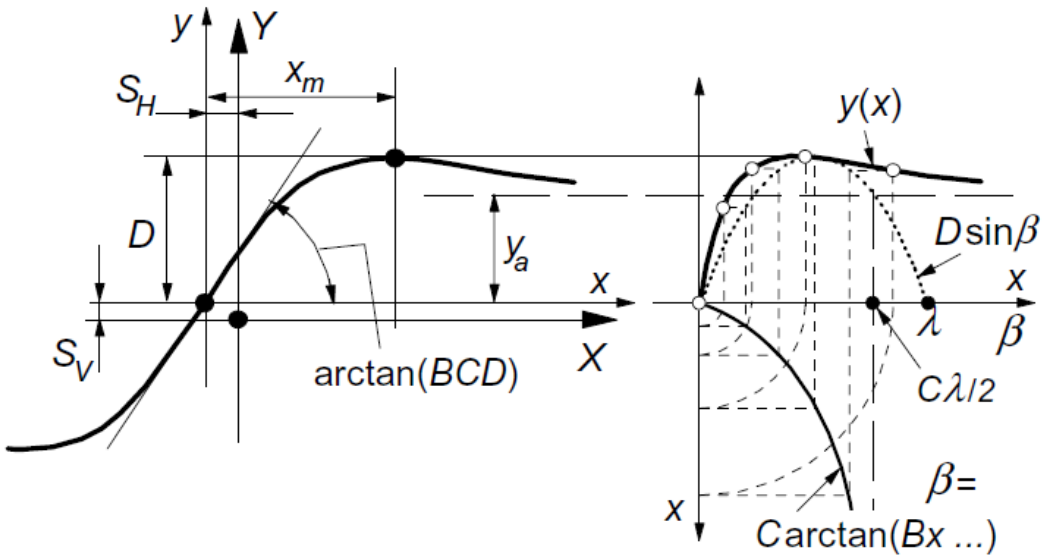

Figure 1.6 Curve produced by the original sine version of the Magic Formula[3]

The magic formula y(x) typically produces a curve that passes through the origin x = y = 0, reaches maximum and subsequently tends to horizontal asymptote.

$$y = Dsin[C \arctan\{Bx - E(Bx - arctanBx)\}]$$

$$Y(X) = y(x) + S_v$$

$$x = X + S_H$$

Where,

Y: output variable F_x, F_y or M_z

X: input variable $tan\alpha$ or κ

And,

B: Stiffness factor

C: Shape factor

D: Peak value

E: Curvature factor

S_H: Horizontal shift

S_V: Vertical shift

For given values of coefficients B, C, D & E, the curve shows an anti-symmetric shape with respect to the origin. To allow the curve to have an offset with respect to the origin, two shifts S_H & S_V have been introduced.

2 Simulator Design

2.1 Components – HW & SW

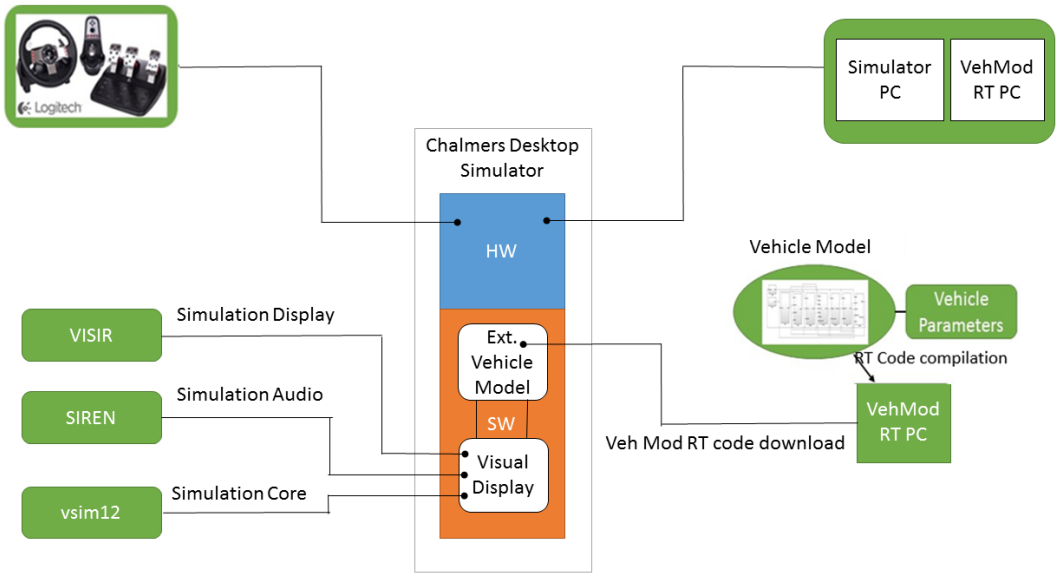

Figure 2.1 Chalmers Simulator structure

Figure 2.1 displays the hardware and software components of the Chalmers desktop simulator.

Hardware –

1. Steering wheel, Pedals, Gear Lever – Logitech G27
2. Simulator PC
3. xPC Target PC – for real time applications

Software –

1. Vehicle Model modelled in Simulink (Simulator PC) compiled for real time usage (xPC target PC).
2. vsim12 project written in Qt Creator communicating with –
    1. Visir – For display
    2. Siren – For audio
    3. Simulation files in vsim12 (core) – For simulation settings

A detailed explanation of the individual components can be found in[1].

2.2 Visual Display Flowchart

As Figure 2.1 illustrates, the simulator software has two parts to it. The external vehicle model is responsible for depicting the dynamic behaviour of the vehicle to be simulated and the visual display takes care of the driver view, scenery and environment models.

A detailed explanation of the external vehicle model will be done in the Section 2.3.

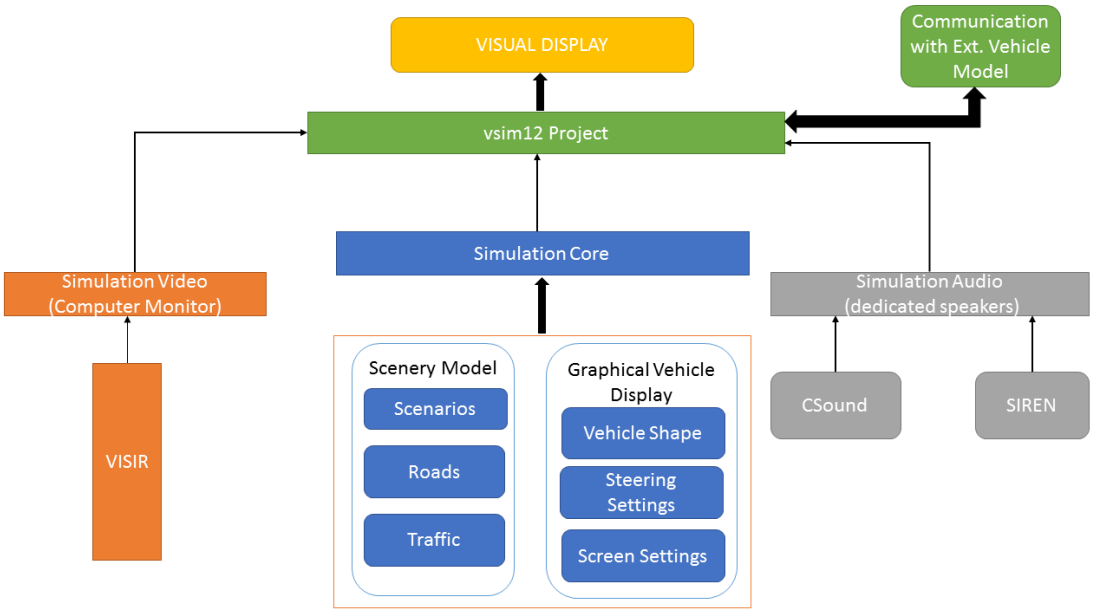

Figure 2.2 Flowchart of Visual Display

The 'visual display' or what the driver can see through the monitor while driving is the output of running the vsim12 project. As shown above, vsim12 has three essential components which interact with each other to simulate the driving experience.

The simulation core represents a number of project files through which a simulation can be controlled and dictated. The settings mentioned under simulation core in Figure 2.2 are just some of the essential files governing a simulation.

The simulation video is provided through an application called Visir which interacts receives input from vsim12 and creates the driver's view while driving.

The simulation audio is created by running two applications namely Csound & Siren in which a predesigned sound file is loaded which replicates the sound of a vehicle (either car or truck). Hence, while driving, at the moment, the engine revving along with wind resistance is audible over the speakers.

2.3 Vehicle Model

2.3.1 Model Communication

The external vehicle model fed into the simulator was originally provided by VTI. It is a double track model with individual subsystems for different components of a vehicle. The vehicle model interacts with the simulator software via xPC target computer to run in real time.

The communication is carried out using UDP (User Datagram Protocol) via LAN cables.

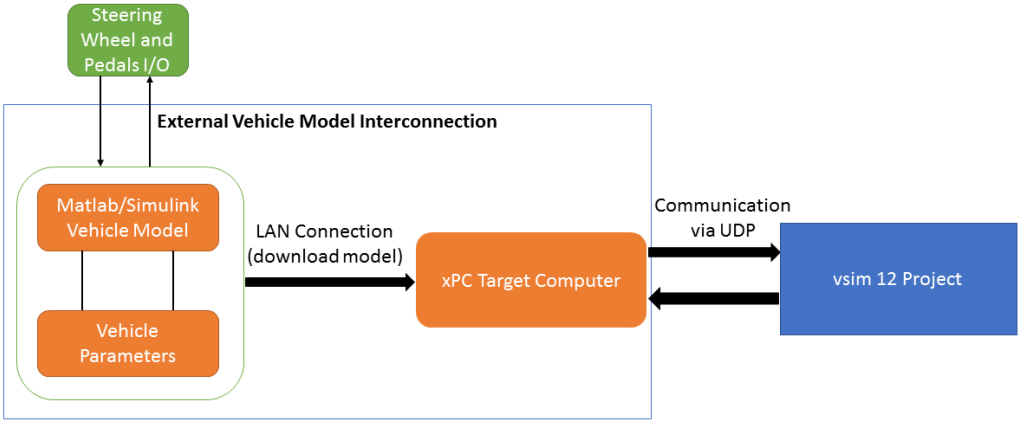

Figure 2.3 Communication – External Vehicle Model

As illustrated in Figure 2.3, the external vehicle model communicates with the vsim12 project (written in Qt Creator) via UDP and uses the IP addresses of both the host and target computers. xPC target is an environment which uses a target PC, separate from the host PC, for running real-time applications[5]. UDP is a transport protocol similar to TCP, however unlike TCP, UDP provides a direct method to send and receive packets over an IP network[5]. UDP uses this direct method at the expense of reliability by limiting error checking and recovery[5].

However, there are other ways of making the simulation run in real time which remove the usage of a 'second' PC. Simulink Coder is a solution which converts the vehicle model directly into readable code for simulator software, however, it couldn't be used in this thesis as it would require more computing time but is a probable solution for future simulations.

The steering wheel and pedals are responsible for the input to the vehicle model along with the vehicle parameters. The entire vehicle model is downloaded onto the xPC target computer and this communicates with vsim12. It can be said that the vehicle model is essentially running on the xPC target computer.

As steering feedback is also calculated in the vehicle model, it is sent back to the steering wheels and its intensity of the different force effects can be dictated using Logitech's steering software.

2.3.2 Model Structure

The vehicle model contains 7 interconnected blocks representing essential vehicle components. The model, itself, has its own set of I/O signals which communicate with vsim12. A complete list of I/O signals is attached as Appendix.

Upon close examination of the logged data, it was concluded that the model follows 'Modified ISO 8855' as a technical standard. The Modified ISO 8855 is quite similar to ISO 8855[23] in many cases except the measurement of tire side slip angles which is considered opposite. Key definitions are described in Appendix D.

The important degrees of freedom considered while modelling were:

- 6x1 DOF – Body (translational & rotational) at COG
- 2x4 DOF – Wheels (rotational and vertical)

Notation – Vehicle Model comprises 7 Blocks (ex. Steer, Wheel, etc)
- Each block has number of subsystems

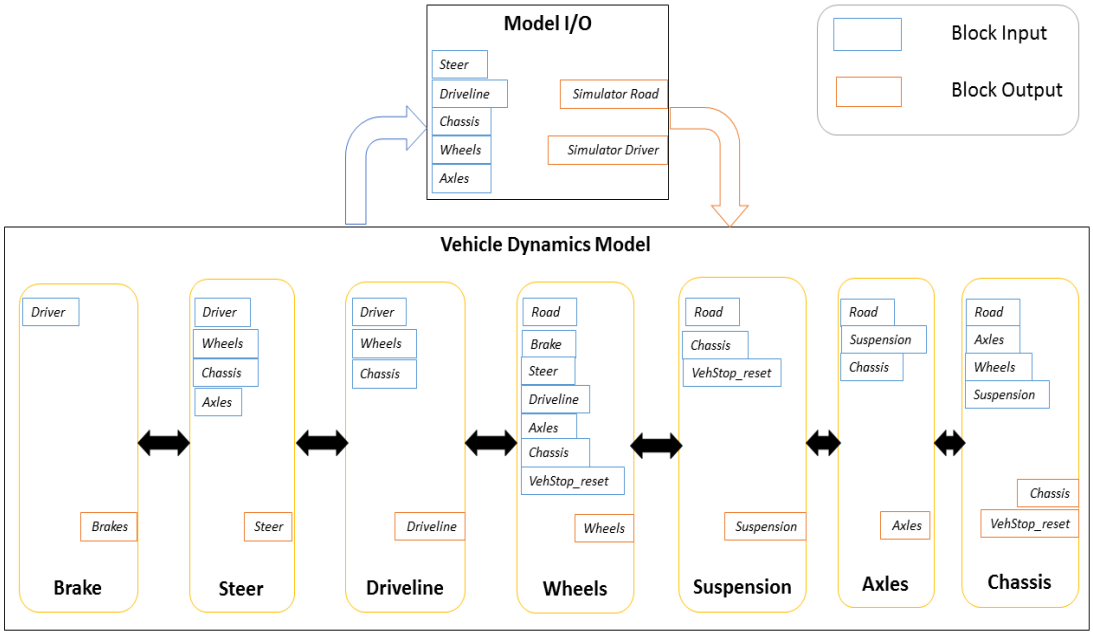

Figure 2.4 Model Overview

As illustrated in Figure 2.4, each block has their individual set of I/O interacting with other blocks in the model. Each block also contains a number of subsystems which help create the final bus signal for the block output. An overview of the various blocks will be given in the next section. Also, the ESC system will be explained in Section 2.3.5

The model has 'guards' to check/reset the simulation when it's completed or displays errors. A watchdog timer is used to perform a system reboot when a programmable timeout occurs[5]. Along with the reset function, the watchdog is responsible for resetting the model to its original state.

Depending on the type of mode, the model I/O is given through Simulink scripts (offline) or through vsim12 (online). This will be further explained in the Section 2.3.4.

2.3.3 Model Blocks

2.3.3.1 Steer Block

The block subsystems are:

- Steering Angle – LF, RF, LR, RR
- Steering Wheel Torque

The steer block uses the steering wheel angle and computes the wheel angles for all 4 wheels and also the steering wheel torque. The model, in its current state, caters for 2 wheel steering so front wheel subsystems receive the steering input to calculate their wheel angles. The model, presently, does not model compliance in steering system.

Besides having no steering input, the rear wheels also have no torsion bar angle. The 'directness' of steering feel during online simulations inspired a need for a simple delay factor to be added to the subsystem while calculating wheel angle.

The formula used to calculate the road wheel angle was -

$$\delta_w = \frac{\delta - angle\_tb}{SG\_ratio} + (F_{y_{tire}} * C_{\delta F_y}) + (M_z * C_{\delta M_z}) + (\emptyset_{mot} * C_{\delta\varphi}) + \psi_{o_{static}} \qquad (2.1)$$

Where,

δ_w = road wheel angle (rad)

angle_tb = Torsion bar angle (rad)

$C_{\delta Fy}$ = Suspension compliance for Lateral Force (rad/N)

$C_{\delta Mz}$ = Suspension torsional compliance (rad/Nm)

$C_{\delta\phi}$ = Roll Steer coefficient

Φ_{mot} = Roll angle due to motion (rad)

The steering coefficients & static toe angle shown in Equation 2.1 are considered for individual axles and are taken from the vehicle parameters. Also the roll steer was calculated using the roll angle due to motion.

As mentioned above, steering wheel torque is another variable calculated in the steer block as a separate subsystem. The steer block is modelled on a servo steering system dependant on speed. Hence, the servo characteristics are provided for three different ranges of velocities.

However, the current model only uses coefficient values for the low speed range as there is a need for parameter tuning for the speed dependant servo steering to be effective. The servo pressure is a function of the steering wheel torque.

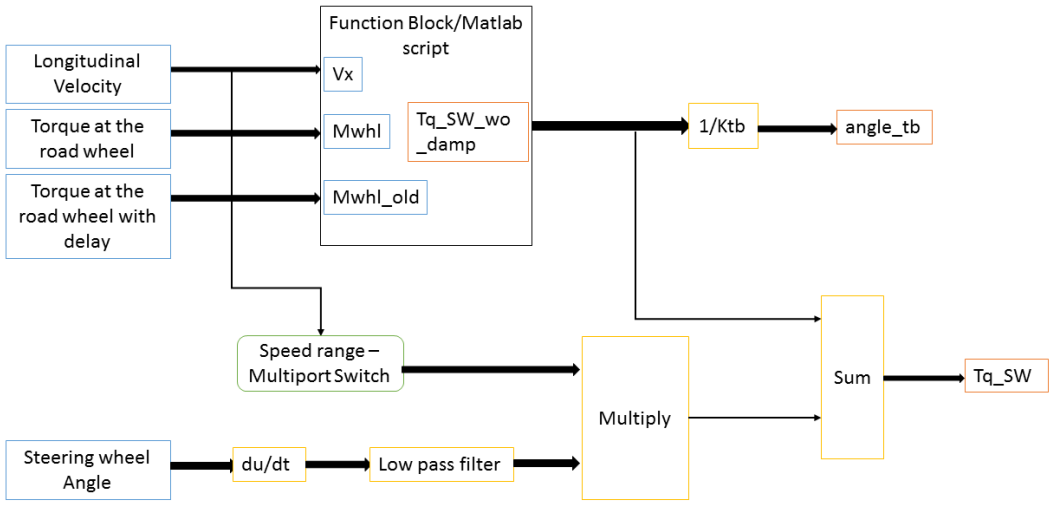

Figure 2.5 Steering Torque structure

The calculation for steering torque (Figure 2.5) is complex as it constitutes calculating the root of a 5^{th} order polynomial so a Matlab script was written to define this. The steering torque considers spring and damper effects in its calculation. However, the feedback experienced in the simulator also incorporates the friction and vehicle inertia effects which can be triggered as required. Since these settings are within the steering wheel equipment, they are not open for the user. This implies that the steering feedback calculated in the vehicle model is received by VTI's software but is not adequately fed to the Logitech steering console due to its construction. The force feedback felt by the driver is manually adjusted through Logitech's console interface. The iterating frequency for force feedback was restricted by the steering wheel's capabilities.

Besides the steering torque, the torsion bar angle is also calculated in the subsystem using the steering torque and torsion bar stiffness.

2.3.3.2 Suspension Block

The block subsystems are:

- Suspension Spring & Damper – LF, RF, LR, RR

The Suspension block represents a simple spring-damper subsystem whose output is the vertical force on each wheel.

Depending on the mode of operation, road profile is fed into this subsystem via vsim12 project (online) or Matlab code (offline). For all offline simulations, the road profile is flat which represents no vertical coordinates. But in the online mode, depending on the road chosen, vertical coordinates maybe provided. The coordinates are extracted for each wheel and sent to respective subsystems.

The coordinates for the wheel positions were calculated from the vehicle's centre of gravity. The front and rear suspensions have different coefficients for spring & damper and along with the tire stiffness' help calculate the vertical loads.

Table 2.1 Parameters for wheels

Description	Symbol	Left Front	Right Front	Left Rear	Right Rear
Longitudinal Position w.r.t CG	a	lf	lf	-lr	-lr
Lateral Position w.r.t CG	b	tw_f/2	-tw_f/2	tw_r/2	-tw_r/2
Unsprung Mass per side	mus	mus_f/2	mus_f/2	mus_r/2	mus_r/2

The equation to calculate vertical load

$$F_{z\_spr\_damp} = \left[\left(\frac{\varphi * (-Karb)}{2b}\right) + \{(Zcg + \varphi * b - \theta * a - Z_w)(-Kspr)\} + \left\{(\dot{Z}cg + \dot{\varphi} * b - \dot{\theta} * a - \dot{Z_w})(-Cdamp)\right\}\right] \quad (2.2)$$

Where,

$F_{z\_spr\_damp}$ = Vertical Spring & Damper Force

2.3.3.3 Driveline Block

The block subsystems are –

- Gearbox
- Clutch
- Engine

The Driveline block receives input signals such as pedal positions, wheel velocities, etc. The model, in its current state, can cater for FWD & RWD vehicles only. However, the 2.8ton Mercedes VitoXL is an AWD vehicle so the model was tuned to incorporate this. This will be explained in Section 2.3.5

The Gearbox subsystem is functional for both manual and automatic transmission. For this thesis, the automatic transmission setting could only be used as the paddles or gear lever positions hadn't been coded into the vsim12 project.

The automatic transmission was designed with a shift logic which simply shifts up or down at certain vehicle speeds. There is no shift delay modelled in the system so the shifting is instantaneous. The velocity settings are taken from the vehicle parameters. As the gear is selected, it would extract the required gear ratio from a look-up table and calculate the total gear ratio via the differential gear. So, depending on which axle is powered, the total gear ratio would be sent to the wheels on that axle.

The Clutch subsystem is a simple system depending on the pedal position provided either by the pedal (online) or written script (offline). While running simulation with automatic transmission it was noticed that the subsystem did not have a model for a torque converter. This could be seen as future work. The clutch position has a range from 0 to 1 wherein a fully pressed pedal would be 1 (clutch disengaged) and 0, a free pedal (clutch engaged). However, the clutch subsystem could not be tested in a manual setting as all simulations were carried out with automatic transmission

Lastly, the Engine subsystem calculates the engine torque based on throttle and engine speed. Starting from the wheel velocities on the left & right, a range of calculation steps (including a low pass filter & speed limiter) are used to calculate the engine speed. For every vehicle, an engine map is fed into the model which calculates the required engine torque for a particular throttle setting.

The driveline block uses a driveshaft moment of inertia value of 0.7 which is used to calculate the complete driveline inertia.

$$I_{drv_{eff}} = I_{drv} + \left(0.5 * I_{eng} * GR_{tot}^2\right) \quad (2.3)$$

Where,

I_{drveff} = Effective Driveline Inertia

2.3.3.4 Brake Block

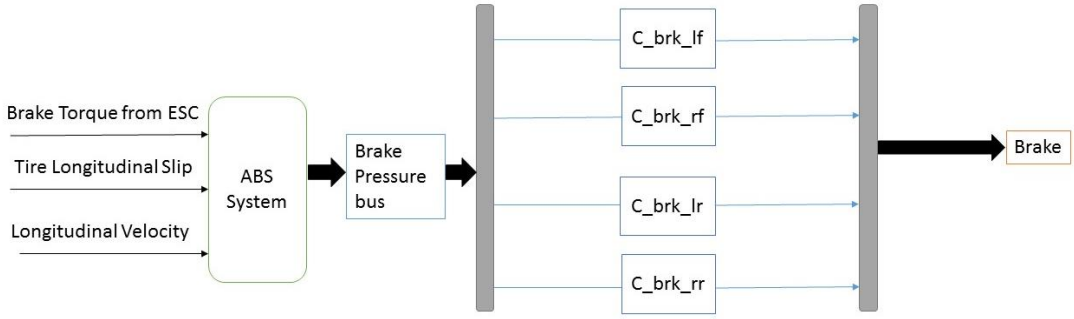

Figure 2.6 Brake block

As Figure 2.6 indicates, the brakes block receives brake pressure for all 4 wheels and uses torque line pressure gradient to convert the pressure into brake torque.

This model does not have an ABS model, hence it was modelled in [1].

2.3.3.5 Wheels Block

The block subsystems are –

- Magic Formula 5.2 – LF
- Magic Formula 5.2 – RF
- Magic Formula 5.2 – LR
- Magic Formula 5.2 – RR

The wheels block, after the chassis block, is the most comprehensively modelled system in this vehicle model. Among inputs from other blocks, it receives inputs such as camber track wall and friction values from vsim12 (road) for its calculations.

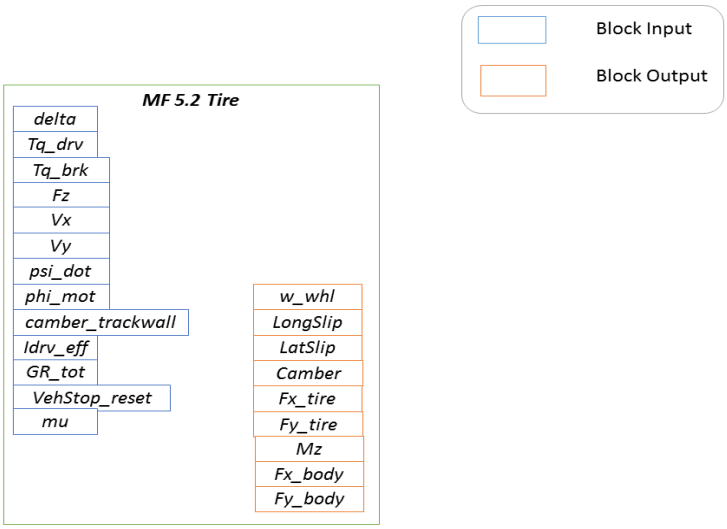

Figure 2.7 Magic Formula 5.2 subsystem

Figure 2.7 shows the I/O to the MF 5.2 subsystem. The MF 5.2 subsystem calculates a number of wheel variables over a particular manoeuvre. Stated below are some of the equations used to calculate the wheel variables -

Wheel rotational speed -

$$\omega_{whl} = \int \dot{\omega}_{whl} = \frac{T_{q\_drv} - T_{q_{brk}} - (F_z * R_w * f_r) - \left(F_{x_{tire}} * R_w\right)}{I_w + I_{drv\_eff}} \tag{2.4}$$

Longitudinal Slip for traction -

$$\kappa = \frac{(\omega_{whl} * R_w) - (V_x + \dot{\psi} * (-b))}{\max\left(abs(\omega_{whl} * R_w), V_{x_{slip}}\right)} \tag{2.5}$$

Longitudinal Slip for braking -

$$\kappa = \frac{(\omega_{whl} * R_w) - \left(V_x + \dot{\psi} * (-b)\right)}{\max\left(V_{x_{slip}}, abs\left(V_x + \dot{\psi} * (-b)\right)\right)} \tag{2.6}$$

Lateral Slip –

$$\alpha_{t1} = \delta - \arctan\left[\frac{V_y + a * \dot{\psi}}{V_x - b * \dot{\psi}}\right] \tag{2.7}$$

$$\alpha_{t2} = \int \frac{V_x(\alpha_{t1} - \alpha_{t2})}{F_z * C_{F\alpha}}$$

Camber Angle –

$$\gamma = \left[\gamma_0 + \gamma_{road} + \left(\varphi_{mot} * C_{\gamma\varphi}\right) + \left(F_{y_{tire}} * C_{\gamma Fy}\right)\right] \tag{2.8}$$

Where,

γ_0 = Static Camber angle (rad)

γ_{road} = Camber Trackwall (rad)

$C_{\gamma\varphi}$ = Roll Camber Coefficient (Front, Rear)

$C_{\gamma Fy}$ = Coefficient for Camber due to lateral force (rad/N) (Front, Rear)

$C_{F\alpha}$ = Tire Cornering Stiffness (N/rad)

The tire forces and aligning torque are calculated using Pacejka's Magic Formula version 5.2 (2001). The MF tire calculates the forces (F_x, F_y) & moments (M_x, M_y, M_z)

acting on the tire under pure & combined slip conditions on arbitrary 3D roads using longitudinal, lateral & turn slip, camber angle & vertical force (F_z) as input quantities[6].

The general form of the formula that holds for given values of vertical load & camber angle reads[3]:

$$y = Dsin[C \arctan\{Bx - E(Bx - arctanBx)\}]$$

$$Y(X) = y(x) + S_v$$

$$x = X + S_H$$

Where,

Y: output variable F_x, F_y or M_z

X: input variable $tan\alpha$ or κ

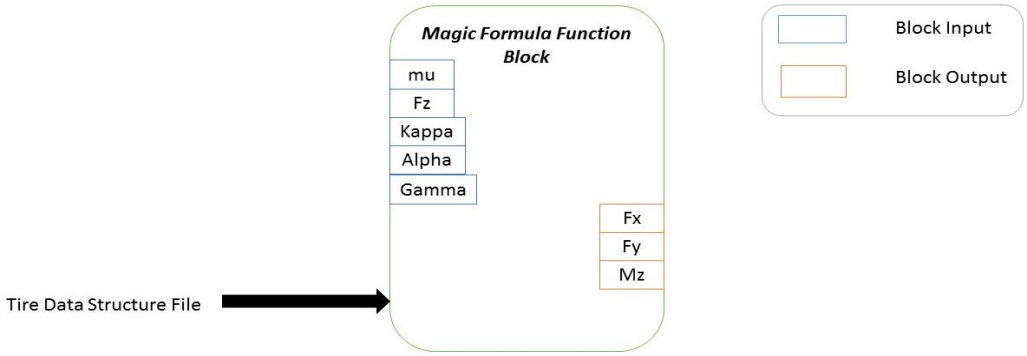

Figure 2.8 Function block – Magic Formula

For this model, Figure 2.8 shows the I/O to the function block. As the magic formula consists of a set of equations along with scaling factors, a Matlab script is fed into the model which lists the magic formula parameters[6] for different road conditions such as dry, wet, snowy, etc.

The function block contains the full set of equations from Pacejka's magic formula. However, turn slip or path curvature is not modelled in the subsystem.

Tire forces in the vehicle body coordinate system –

$$F_{x_{body}} = (F_{x_{tire}} * \cos\delta) - (F_{y_{tire}} * \sin\delta) \quad (2.9)$$

$$F_{y_{body}} = (F_{x_{tire}} * \sin\delta) + (F_{y_{tire}} * \cos\delta) \quad (2.10)$$

Where,

$F_{x\ body}$ = Longitudinal Tire Force in vehicle body coordinate systems (N)

$F_{y\ body}$ = Lateral Tire Force in vehicle body coordinate systems (N)

2.3.3.6 Axles Block

The block subsystems are –

- Axle Load – Front
- Axle Load – Rear

The vertical load on each wheel on an axle is a combination of different loads acting on the wheel.

For front axle,

$$Sprung\ Mass = ms_{front} = \frac{ms * lr}{lf + lr} \tag{2.11}$$

$$static\ load = \left(ms_{front} + mus\_f\right) * g \tag{2.12}$$

For rear axle,

$$Sprung\ Mass = ms_{rear} = \frac{ms * lf}{lf + lr} \tag{2.13}$$

$$static\ load = (ms_{rear} + mus\_r) * g \tag{2.14}$$

This implies,

Right wheel -

$$F_{z_{right}} = \left[\left(0.5 * static\ load * \cos\left(Ave_{slope}\right)\right) + F_{z\_spr\_damp\_right} + \left(a_y \frac{(ms*hr+mus*hus)}{tw}\right)\right] \tag{2.15}$$

Left wheel,

$$F_{z_{left}} = \left[\left(0.5 * static\ load * \cos\left(Ave_{slope}\right)\right) + F_{z\_spr\_damp\_left} - \left(a_y \frac{(ms*hr+mus*hus)}{tw}\right)\right] \tag{2.16}$$

2.3.3.7 Chassis Block

The block subsystems are –

- Speed & Acceleration Calculation
- Yaw Calculation
- Roll Calculation
- Pitch Calculation
- Vertical Movement of CG
- Position in global coordinate

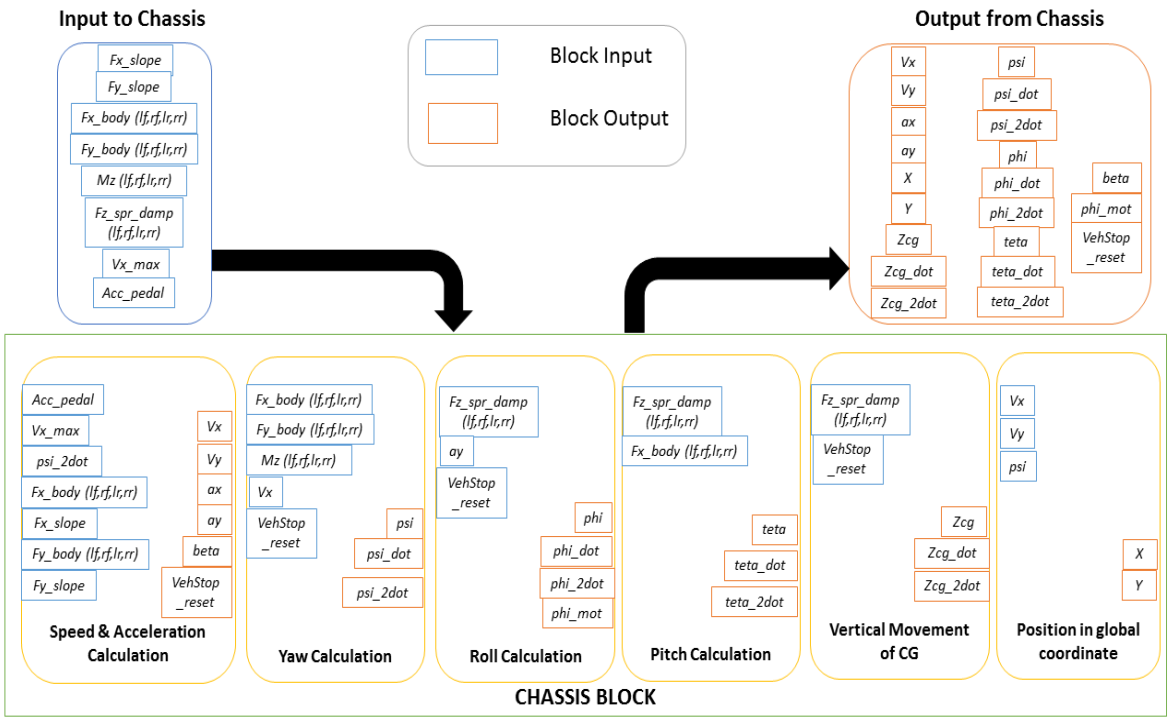

Figure 2.9 Chassis block

All the subsystems labelled above calculate the essential variables to study the vehicle state in terms of vehicle position (in x & y), movement (in x, y & z) & rotation (in x, y, & z).

The various equations used in the model are –

$$F_{x\_slope} = Ave_{slope} * (-m * g) \tag{2.17}$$

For vehicle velocities,

$$F_{x\_air} = 0.5 * \rho * Cax * A0 * V_x^2 \tag{2.18}$$

$$V_x = \int \dot{V}_x = \left[\left(V_y * \dot{\psi} \right) + \frac{1}{m} \left(F_{x\_body\_lf} + F_{x\_body\_rf} + F_{x\_body\_lr} + F_{x\_body\_rr} + F_{x\_air} + F_{x\_slope} \right) \right] \tag{2.19}$$

$$V_y = \int \dot{V}_y = \left[\frac{1}{m} \left(F_{y\_body\_lf} + F_{y\_body\_rf} + F_{y\_body\_lr} + F_{y\_body\_rr} + F_{y\_slope} \right) - \left(V_y * \dot{\psi} \right) \right] \tag{2.20}$$

For vehicle acceleration,

$$a_x = \frac{1}{m} \left(F_{x\_body\_lf} + F_{x\_body\_rf} + F_{x\_body\_lr} + F_{x\_body\_rr} + F_{x\_air} + F_{x\_slope} \right) \tag{2.21}$$

$$a_y = \frac{1}{m} \left(F_{y\_body\_lf} + F_{y\_body\_rf} + F_{y\_body\_lr} + F_{y\_body\_rr} + F_{y\_slope} \right) \tag{2.22}$$

With reference to Table 2.1 –

Vehicle yaw angle,

$$\psi = \int \dot{\psi} = \int \ddot{\psi} = \left[\frac{1}{I_z}\{(F_{y\_body\_lf} * a_{lf}) + (F_{y\_body\_rf} * a_{rf}) + (F_{y\_body\_lr} * a_{lr}) + (F_{y\_body\_rr} * a_{rr}) - (F_{x\_body\_rr} * b_{rr}) - (F_{x\_body\_lr} * b_{lr}) - (F_{x\_body\_rf} * b_{rf}) - (F_{x\_body\_lf} * b_{lf}) + M_{z\_lf} + M_{z\_rf} + M_{z\_lr} + M_{z\_rr}\}\right] \quad (2.23)$$

Vehicle roll angle,

$$\varphi = \int \dot{\varphi} = \int \ddot{\varphi} = \left[\frac{1}{I_r}\{(F_{z\_spr\_damp\_lf} * b_{lf}) + (F_{z\_spr\_damp\_rf} * b_{rf}) + (F_{z\_spr\_damp\_lr} * b_{lr}) + (F_{z\_spr\_damp\_rr} * b_{rr}) + (a_y * ms * hsr) + (\varphi * ms * hsr * g)\}\right] \quad (2.24)$$

Vehicle pitch angle,

$$\theta = \int \dot{\theta} = \int \ddot{\theta} = \left[-\frac{1}{I_y}\{(F_{z\_spr\_damp\_lf} * a_{lf}) + (F_{z\_spr\_damp\_rf} * a_{rf}) + (F_{z\_spr\_damp\_lr} * a_{lr}) + (F_{z\_spr\_damp\_rr} * a_{rr}) + (0.8 * h_{cg}(F_{x\_body\_lf} + F_{x\_body\_rf} + F_{x\_body\_lr} + F_{x\_body\_rr}))\}\right] \quad (2.25)$$

Vertical movement of CG,

$$Z_{cg} = \int \dot{Z_{cg}} = \int \ddot{Z_{cg}} = [\frac{1}{ms}(F_{z\_spr\_damp\_lf} + F_{z\_spr\_damp\_rf} + F_{z\_spr\_damp\_lr} + F_{z\_spr\_damp\_rr})] \quad (2.26)$$

Position in global coordinates,

$$X = \int V_{x\_global} = \left[(V_x * \cos\psi) - (V_y * \sin\psi)\right] \quad (2.27)$$

$$Y = \int V_{y\_global} = \left[(V_y * \cos\psi) + (V_x * \sin\psi)\right] \quad (2.28)$$

2.3.4 Offline & Online model structure

The offline and online structures differ in the way they provide I/O for the vehicle model.

2.3.4.1 Offline Model

The I/O for offline mode comprises of 2 subsystems –

- Driver
- Road

The output signals shown in both these subsystems are coded in Matlab and depending on the offline manoeuvre, different inputs can be fed.

The vehicle model doesn't contain a 'typical' driver model as it just supplies the intended driver output signals to the vehicle model (open loop). For the offline model, no stimulus is provided to the driver but with a proper driver model, stimulus can be created to increase levels of realism.

The signals in the Driver subsystem are shown in Table 2.2

Table 2.2 – Output signals from driver to model

S.No	Signal Name	Unit	Description
1.	reset	-	Step signal
2.	SWA_in	[rad]	Steering wheel Angle
3.	throttle_in	-	Acceleration Pedal (0-1)
4.	clutch_pedal	-	Clutch Pedal (0-1)
5.	gear_manual	-	Manual Gear
6.	BRK_lf_in	[Pa]	Brake Pressure LF
7.	BRK_rf_in	[Pa]	Brake Pressure RF
8.	BRK_lr_in	[Pa]	Brake Pressure LR
9.	BRK_rr_in	[Pa]	Brake Pressure RR
10.	Vx_max	[m/sec]	Max. Longitudinal Velocity
11.	auto_gear	[]	Automatic Gear Flag

All the signals stated in Table 2.2 are compiled from a Matlab script or prescribed in the vehicle parameters. This replaces the actual input typically provided by a driver in

a real car. But in the case of brakes, instead of brake position, brake pressure is supplied to the model.

The offline simulations for this thesis will be further elaborated upon in Section 4.1.1.

The signals in the road subsystems are shown in Figure 2.10. The feedback provided to the road subsystem is the vehicle position in X direction based on the global coordinate system. However, with a 'dedicated' road model, the input signals to the road model can arbitrarily range from no input signals (constant road) to signals modelled depending on the definition of the surrounding environment the vehicle is.

Figure 2.10 Road subsystem

$$Ave\ slope = \left[\frac{1}{4}\left(dzdx_{lf} + dzdx_{rf} + dzdx_{lr} + dzdx_{rr}\right)\right] \quad (2.29)$$

Table 2.3 – Signals from road to model

S.No	Bus Name	Signal	Description
1.	LF, RF, LR, RR	z	Road coordinate in z-direction
		dzdx	Road coordinate in z-direction with respect to x
		dzdy	Road coordinate in z-direction with respect to y
		camber_trackwall (γ_{road})	Camber angle due to inclination of road
2.	Ave slope		Average slope of road
3.	mu	LF	Coefficient of friction (tire – road)
		RF	
		LR	
		RR	

For the simulations in this thesis, the road coordinates are assumed for a level road with no banking or inclination angles & dry conditions. Hence, the coefficient values for tire-road friction are set as 1.

2.3.4.2 Online Model

The online model communicates with the simulator software (vsim12 project written on Qt Creator) and is the one used for all the online simulations in this thesis. Hence, the road and driver inputs to the model are received from vsim12 through UDP packets (refer Figure 2.3) and certain variables are transmitted back to vsim12 from the model. A complete list of vehicle I/O is attached as Appendix A.

The relative position and orientation of the test driver in the simulated vehicle is added in vsim12. A total of 6 parameters (scalar) are written in an xml file (frame.xml) on the project along with the relative position & orientation of the simulator screen(s) and the rear view mirrors. Besides this, the physical position of the driver from the simulator screen and the gaze angle can also be fed into frame.xml.

In comparison with the offline model, there is more feedback provided to vsim12 in the online model. The feedback is provided from model blocks such as Steer, Driveline, Chassis, Wheels and Axles (refer Figure 2.4 for I/O structure). This is mainly done, among other things, for data logging. Total number of signals logged are 138, however a lot of the variables are logged more than once, hence a rough number would be close to 100.

The data communication takes place with the help of two subsystems, namely, UDP I/O and UDP processing. In UDP processing, feedback signals from the model are combined to create a bus signal called UDP output. Also the input signals to the model from vsim12 are combined to create the UDP input bus signal. In UDP I/O, the packing and unpacking of the bus signals takes place.

A Matlab script is written to indicate the simulator communication parameters such as port numbers, simulation time step, etc. For this thesis, the number of signals received from vsim12 is restricted to 35. These signals include steering wheel angle, accelerator pedal position, etc.

2.3.5 Electronic Stability Control system

The Electronic stability control system used in this thesis is taken as a reference from a student thesis[7] conducted on the Chalmers Motion Platform simulator (S2) and adapted to the vehicle model. A detailed description of the system can be found in[7].

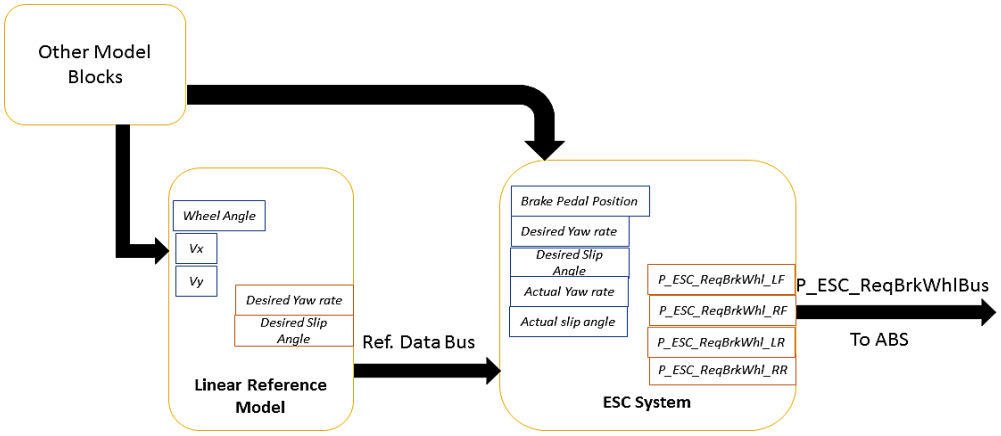

Figure 2.11 ESC Overview

The ESC system is designed as a yaw control by brake system which is a common system designed for understeer - oversteer mitigation. The ESC system designed for the Chalmers Motion Platform Simulator (S2) implements yaw control as well as side slip control. It uses a single track bicycle model as the linear reference model to compute the desired yaw rate and side slip.

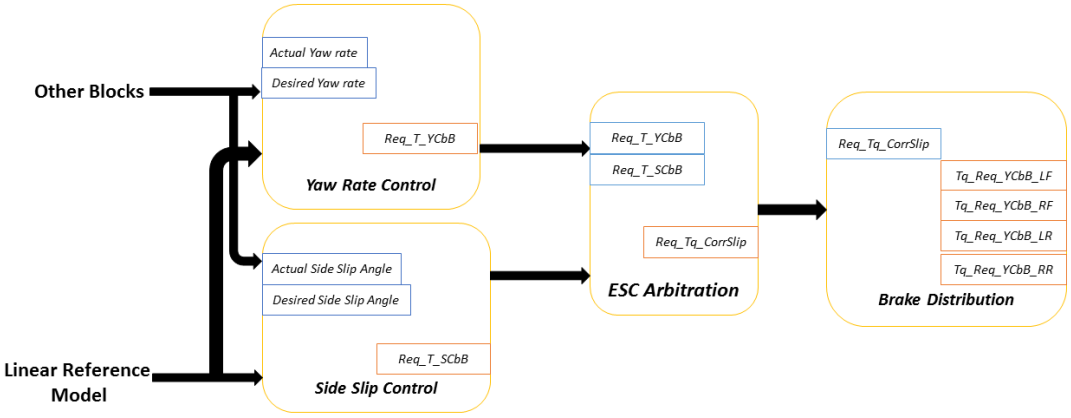

Figure 2.12 ESC Structure

With reference to Figure 2.12, the actual and desired values are compared and fed into a PD controller to compute the required torque. The required torques from the yaw rate control and side slip control are arbitrated to determine 'superiority' and the correctional torque is finally distributed to the wheels depending on the brake distribution.

For this thesis, the side slip control was switched off and emphasis was laid on the yaw rate control. This then skips the arbitration and computes brake torque directly from he requested torque from the yaw control system.

2.3.6 Parameterised Models – Ambulances

A combination of generic values & scaling of parameters was adopted to play a key role for the parameterisation of the ambulance vehicles. An attempt was made to determine the least number of parameters, which when scaled, influence the vehicle behaviour. As the parameters of the S40 were deemed accurate and the model accordingly parameterised, parameters for the ambulances were scaled using this.

The total number of parameters demanded by the external vehicle model are about 75. The chosen parameters which were used to scale the remaining parameters are:

Scaling Parameters:

1. Vehicle Mass, *m*
2. Vehicle wheel base, *wb*
3. Wheel radius, R_w
4. Centre of Gravity height, h_{CG}

Table 2.4 – Scaled variables

Vehicle Parameter	Scaled with
Vehicle Mass (Sprung, Unsprung)	m
Vehicle Moment of Inertia (I_x, I_y, I_z)	m
Unsprung Mass Height (F & R)	h_{CG}
Axle Distances (F & R)	wb
Wheel rotational Inertia	R_w^2
Tire (Stiffness, Damping & Lateral Stiffness)	m*g
Suspension Coefficients (Spring, Damper, Anti-Roll)	m*g
Roll Axle Height (F & R)	h_{CG}
Steering Gear Ratio	wb
Torsion bar stiffness	wb
Drive shaft Moment of Inertia	m

Table 2.4 indicates a certain set of parameters which were scaled according to the chosen parameters. To complete the remaining parameters, values from a typical van[4] were considered.

2.3.6.1 Non-Generic parameterization

As mentioned in Section 1.1.4, the Mercedes VitoXL & Sprinter vans were utilised as test vehicles. The main modifications made to the vehicle model, additional to the scaling described above are:

a. Steering Block

- Delay function to steering input as steering sensitivity was perceived to be high during online driving – by VTI

- The steering system incorporated in this model was a servo steered speed dependant rack & pinion system. As the servo characteristic curves were restricted to low speed velocity range, a certain level of parameter tuning was carried out to approach a perceivable range of steering torque.

b. Driveline Block

- Engine – As engine specs for OM 651 powering the ambulances weren't complete, a generic torque speed curve of the OM651[22] used in the Mercedes C-Class was used and scaled up to the rated torque and speed conditions of the ambulances.

c. Wheels Block

- As the model uses the Magic Formula 5.2 to calculate the tire forces, the tire coefficients were modified/scaled with reference to the typical van[4] & the base vehicle.

3 Simulator Scenarios

The simulation scenarios are chosen such that they supplement the scenarios as suggested by representatives from VGR. The simulations are structured in such a way that they provide information to answer the research questions stated earlier in the thesis. Contemplating driver behaviour for the advanced case, straight line braking, sine with dwell and double lane change tests were chosen, see Table 3.1.

As stated in Section 1.1.4, a base vehicle (Volvo S40) was used to judge the working of the active safety systems. It was assumed that, as the vehicle model was received with the base vehicle parameters, it is parameterised to the S40 and displays accurate results.

Table 3.1 – Vehicle & Simulation Type for given manoeuvre

Driving Manoeuvre	Type of Simulation	Test Vehicles	Active Safety System
Obstacle Avoidance (see Section 1.1.5)	Online	Mercedes Sprinter	ESC+ABS
Straight Line Braking, SLB	Offline & Online	S40 & Mercedes Sprinter	ABS
Sine with Dwell, SWD	Offline	S40 & Mercedes VitoXL	ESC+ABS
Double Lane Change, DLC	Online	Mercedes VitoXL	ESC+ABS

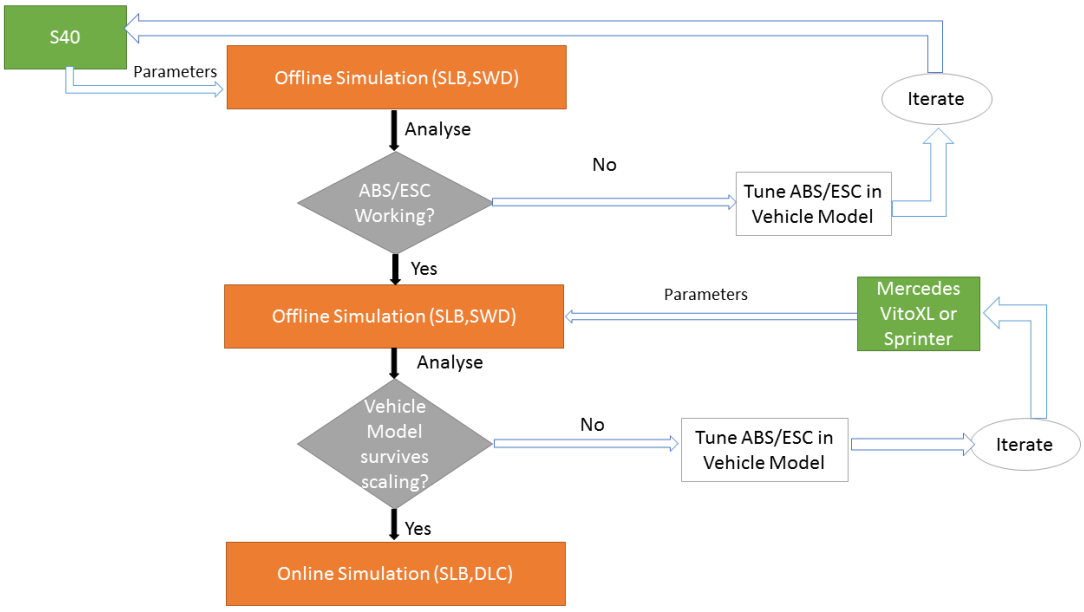

Figure 3.1 Simulation Flowchart

Referring to the research questions 1 & 2 in Section 1.1.2, a simulation flowchart was prepared (Figure 3.1) which shows the decision making plan used for the simulations. The important questions asked are –

For ABS

1. Does ABS work with the base vehicle?
    a. Plot X(t) – with/without ABS
    b. Plot $V_x(t)$ – with/without ABS
    c. Plot $\kappa(t)$ – with/without ABS (LF,RF,LR,RR)
    d. Plot V_x & ω_{whl} vs time – with/without ABS (LF,RF,LR,RR)

2. Does ABS survive parameterization/scaling with the test vehicle? (same plots as above)

3. Does ABS function when shifting to online simulation? (same plots)

For ESC

1. Does ESC work with the base vehicle? – see Appendix C
    a. Plot X vs Y – with/without ESC
    b. Plot $V_x(t)$ – with/without ESC
    c. Plot $\dot{\psi}(t)$ – with/without ESC
    d. Plot $\dot{\varphi}(t)$ – with/without ESC.

2. Does ESC survive parameterization/scaling with the test vehicle? (same plots as above)

3. Does ESC function when shifting to online simulation? (same plots)

3.1 Obstacle Avoidance

As the ASTAZero graphical environment for the simulator wasn't operational during the thesis, the tests were carried out on sample roads provided by VTI. The obstacle avoidance scenario was simulated on the 'rural_1' road environment as specified by VTI.

The modified scenario recreates the original scenario (Section 1.1.5) using position triggered cones which replace the function of the balloon car.

The 'element of surprise' in the original scenario established by the visual obstruction will be replaced by position triggering in the modified scenario. If timed accurately, it should be able to recreate the same driving situation/behaviour.

When faced with such a driving situation, the driver would either proceed with a full brake condition or perform a lane change in order to negotiate the car/cones.

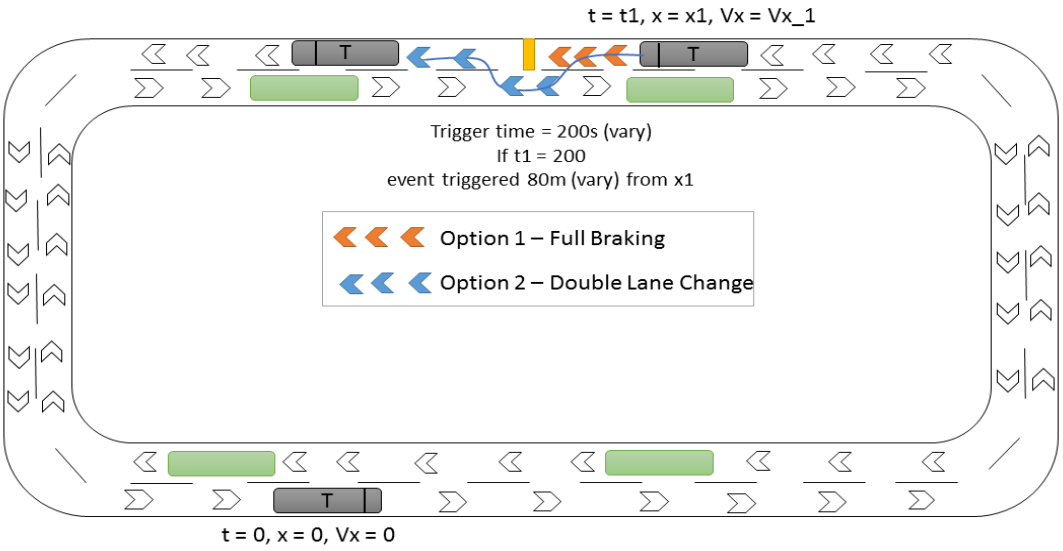

Figure 3.2 Obstacle Avoidance

The 'rural_1' road environment chosen for this manoeuvre is also a looped track with a typical rural setting. Oncoming traffic contributes to the driver's decision making when the scenario is triggered. For this thesis, position triggering couldn't be achieved so time triggering was used to trigger the cones after a stipulated amount of time. This time was compounded after repeated tests on the road environment to determine the best suitable position depending on the relative vehicle speed.

E.g. Time trigger = 200s, so as the simulation time crosses 200s, the cones are placed 80m away from the vehicle's position at t = 200s. It is possible to optimize the position of the cones from the car through repeated iterations of the scenario and depending on relative vehicle speed. This would influence the vehicle to perform full braking or lane change manoeuvres as the best optimized solution to avoid collision.

3.2 Simulation Tests

3.2.1 Straight Line Braking ISO 21994

The stopping distance of a road vehicle is an important part of vehicle performance & active safety[21]. The straight line braking test represents an important test to gauge the longitudinal behaviour of a vehicle.

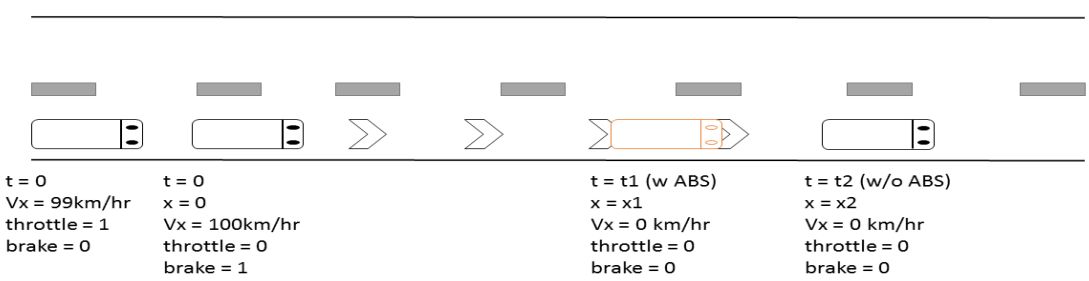

Figure 3.3 Straight Line Braking

This tests was performed in collaboration with another student thesis[1]. A detailed description of the ABS system can be found in[1].

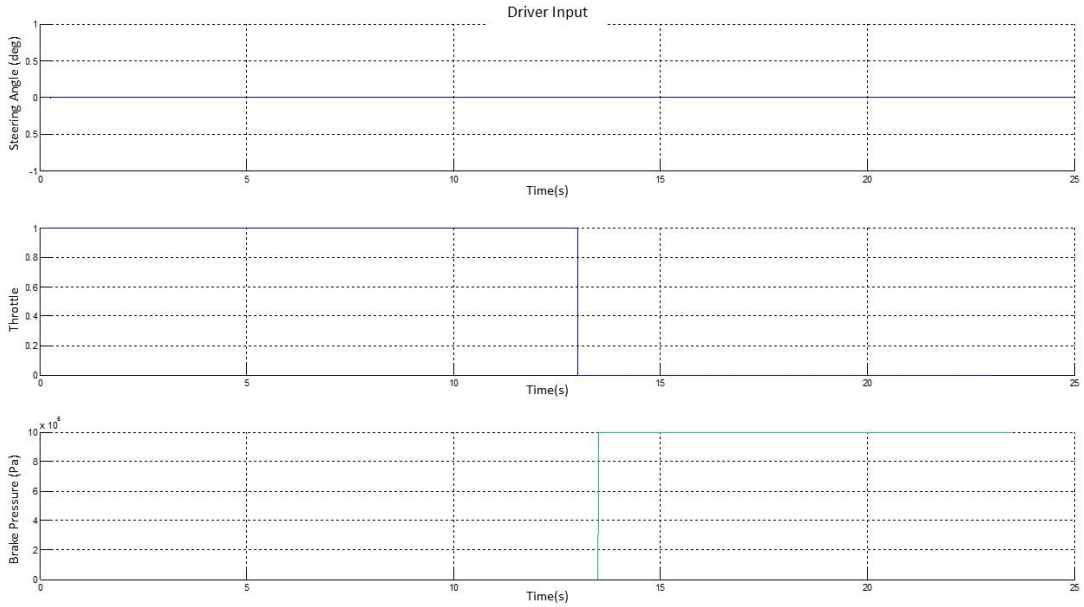

Figure 3.4 Offline Driver Input - Straight Line Braking (S40)

The straight line braking test requires the driver to achieve a set speed of 100 km/h within the shortest possible time with a speed margin of 2 km/h. As two vehicles (S40 and Mercedes Sprinter) are to be tested, after repeated tests, a suitable 0-100 km/h time was determined for each of them and fed in the driver input. Total simulation time was 20 sec.

A delay time of 0.5 sec was provided between throttle off and brake on, to attempt a realistic driver response time. A maximum brake pressure of 100 bar at full brake (for cars) was used.

3.2.2 Sine wave with Dwell (SWD) TP-126-03

In the case of Sine wave with Dwell, the manoeuvre settings are seen in Table 3.2

Table 3.2 – SWD settings

SWD Setting	Values
Turn Frequency	0.7
Pre – Test velocity	87 km/h
Amplitude Test	2*90*pi/180
Time pause (dwell)	500 ms
Test Velocity	80 km/h
Total simulation time	15 sec

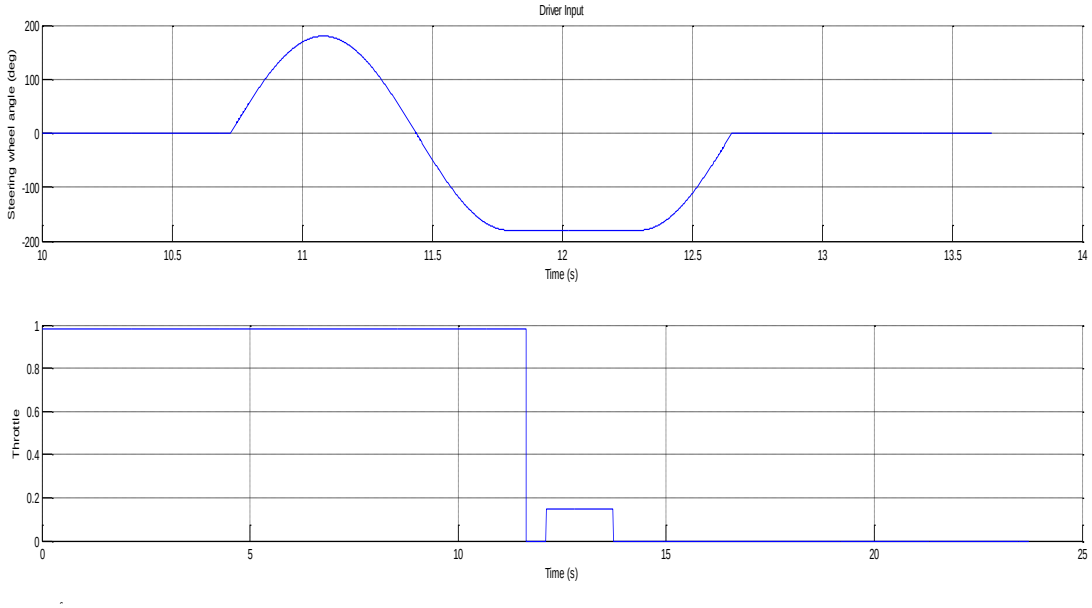

Figure 3.5 Offline Driver Input Test 2 – Sine wave with Dwell (S40)

The SWD tests were performed offline for two different steering amplitudes. For the 1st test, the simulation settings are set according to ISO standards[14] as shown in Table 3.2. This test was carried out so as to determine whether the ESC intervenes to stabilise the vehicle or not.

To visualize the ESC performance to a greater extent, the steering amplitude was doubled in Test 2. This renders the vehicle highly unstable and shows ESC mitigation more clearly. Simulation results for Test 2 have been discussed in Section 4.2.

3.2.3 Double Lane Change – ISO 3888-1

It was difficult to recreate the SWD manoeuvre online. Hence, the double lane change manoeuvre was chosen as both are evasive driving manoeuvres and have certain similarities. The online simulations weren't performed by professional drivers, but it serves our purpose of seeing ESC intervene when needed.

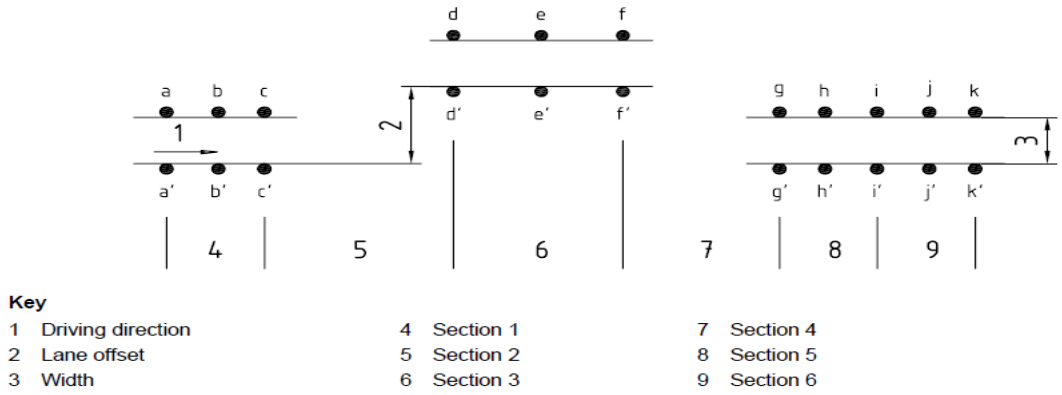

Figure 3.6 Placing of cones for DLC track[16]

Table 3.3 Dimensions of DLC track[16]

Section	Length	Lane Offset	Width
1	15	-	1.1 * vehicle width + 0.25
2	30	-	-
3	25	3.5	1.2 * vehicle width + 0.25
4	25	-	-
5	15	-	1.3 * vehicle width + 0.25
6	15	-	1.3 * vehicle width + 0.25

The DLC track was setup as shown in Figure 3.6 according to the dimensions specified in Table 3.3. The dimensions of the cones were set according to ISO standards[16].

According to VTI's software, the vehicle shape is specified from the external vehicle model but also in the software itself. However, the vehicle width used to specify the dimensions of the track is from the external vehicle model. The chosen drivers were advised to keep an entry velocity, for section 1, as 80 km/h. This was deemed sufficient to investigate ESC mitigation.

4 Simulation Results

The simulation results were compiled following Table 2.3 and the flowchart in Figure 3.1.

4.1 Obstacle Avoidance

With reference to Section 3.1, the obstacle avoidance scenario was carried out with multiple drivers. Data logging was not considered necessary as the evaluation was more subjective than objective. In the original scenario (Section 1.1.5), the test driver is to be evaluated with respect to his response time and chosen 'avoidance' measure. A driver trainer discusses the 'ideal' possible behaviour with the test driver with respect to a particular scenario and provides feedback for the overall drive.

As this 'modified' obstacle avoidance was constructed to give an idea about the braking and yawing behaviour of the ambulance vehicle model, it influenced the ABS and ESC model tuning. As mentioned in Section 3.1, positioning of the cones was varied to test the full brake condition, i.e. vehicle stopping distance & time in the offline mode. With a cone position of 60m from vehicle, full brake must stop the vehicle around 25m before the cone for the ideal stopping distance (referring to Table 4.1). However, with the current ABS tuning, the vehicle stopped 10m before the obstacle.

ESC mitigation was more difficult to investigate as, most of the test drivers chose to brake rather than swerve away from the obstacle. However, when advised to swerve instead of brake, the vehicle velocity was too low to see any significant intervention. Moreover, as will be explained in Section 4.4, the single lane change or double lane changes are influenced by driver skill.

4.2 Straight Line Braking

For the straight line braking test, technical specifications regarding the acceleration time and stopping distance were comprehended. While parameterizing, an approach was made to achieve similar values to validate changes made in the vehicle model. The acceleration/braking specs are as follows -

Table 4.1 Vehicle Specs

Vehicle	**Active Safety Systems**	**Time (0-100 km/h)**	**Stopping Details (100-0 km/h)**
Volvo S40 2L (2007)	ABS, EBD, EBA, DSTC	9.5s	37m in 3.5s (from specs)
Mercedes Sprinter 3L (2013)	Adaptive ESC (ABS, EBD, BAS, ASR)	10.3s	34.3m in 4s (from track testing)

It must be noted that exact values may not be achievable owing to the various systems co-interacting with each other in an actual car.

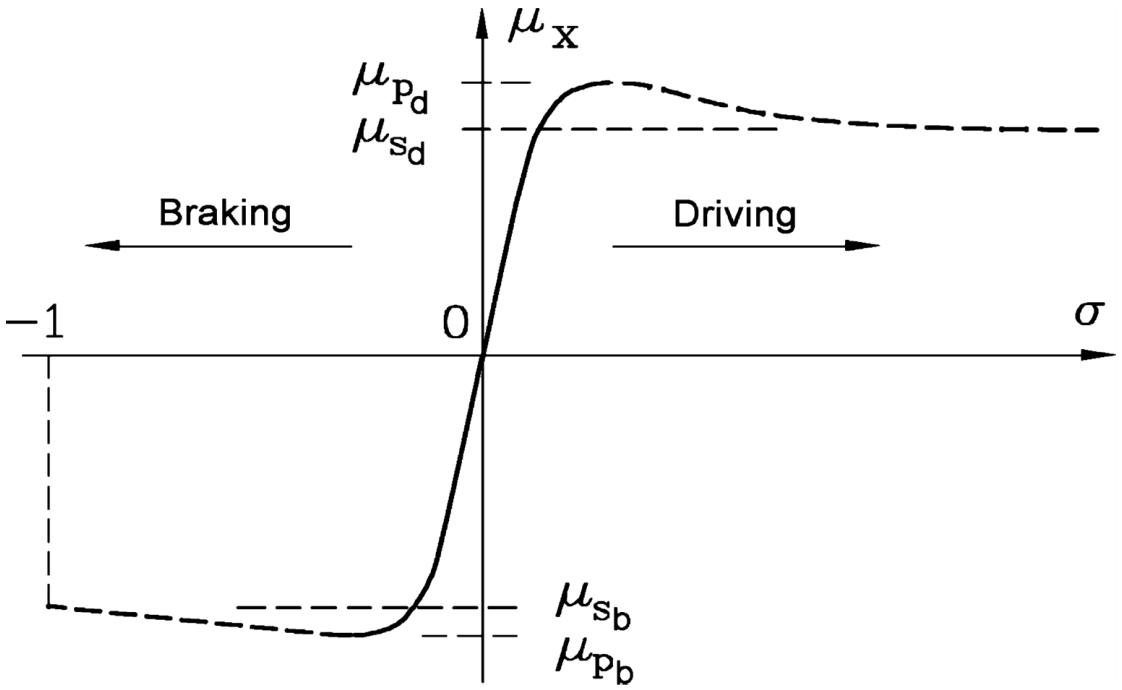

Figure 4.1 Longitudinal Force Coefficient as a function of longitudinal slip[4]

$$Longitudinal\ Force\ Coeff, \mu_x = \frac{F_x}{F_z} \tag{4.1}$$

Where,

μ_{sb} = Sliding value of longitudinal force coefficient

μ_{pb} = Peak value of longitudinal force coefficient

Figure 4.1 illustrates the non-linear relationship of the longitudinal force with slip. For the full brake condition, as the traction approaches its peak value, the force decreases and the wheel tends to lock (quickly). This reduction of tractive force, besides causing slipping (state of combined slip), also effects the handling and stability of the vehicle.

Hence, the load transfer from the rear axle to the front axle can be computed by[3],

$$\Delta F_z = \frac{h_{COG}}{l} F_L \ , (at\ low\ speeds) \tag{4.2}$$

$$F_{z1} = F_{z1,static} + \Delta F_z, \quad F_{z2} = F_{z2,static} - \Delta F_z \tag{4.3}$$

Where,

F_L = Longitudinal force corresponding to inertial force at braking

During braking, the suspension prevents the load transfer from the rear to the front from being too rapid and thus when the vehicle begins to brake, the vertical loads are the same as those at constant speed.

Due to the dynamic load transfer, the cornering stiffness's & peak side forces for the front and rear change, increasing at the front, reducing at the rear. Locking of the rear wheels causes the vehicle to become unstable (extreme oversteer – fish tail) and locking

of the front wheels makes the vehicle uncontrollable (extreme understeer), i.e. travel on a straight trajectory.

To establish a relationship between the braking moments for the front and rear wheels, a ratio is defined[4]

$$K_b = \frac{M_{b1}}{M_{b2}} \tag{4.4}$$

Hence, the total braking force acting on the vehicle when the wheels lock[4],

When rear wheels lock,

$$F_{x1} + F_{x2} = F_{x2}(1 + K_b) \tag{4.5}$$

When front wheels lock,

$$F_{x1} + F_{x2} = F_{x1}\left(1 + \frac{1}{K_b}\right) \tag{4.6}$$

It is highly important for the ABS to intervene on all four wheels to prevent such a condition.

4.2.1 Volvo S40 2L (2007)

As mentioned before, a Volvo S40 was used as the base vehicle to test the functioning of the ABS.

Table 4.2 ABS Simulation Settings (S40)

ABS Settings	Values
Desired Slip	-0.15
Backlash (Deadband width)	0.0001
Controller Gain (I)	6
Controller Gain (P)	15

The ABS system was designed such that when the controller detects the longitudinal tire slip to be nearing the desired value, the ABS kicks in and mitigates the brake torque till the tire slip reaches a lower value. It mitigates to confine the wheel slip to remain within a narrow range around the slip value. A backlash setting was added to prevent the ABS controller from acting too much, too fast.

The following plots display the extent at which the ABS controls the tire slip and prevents the wheels to lock.

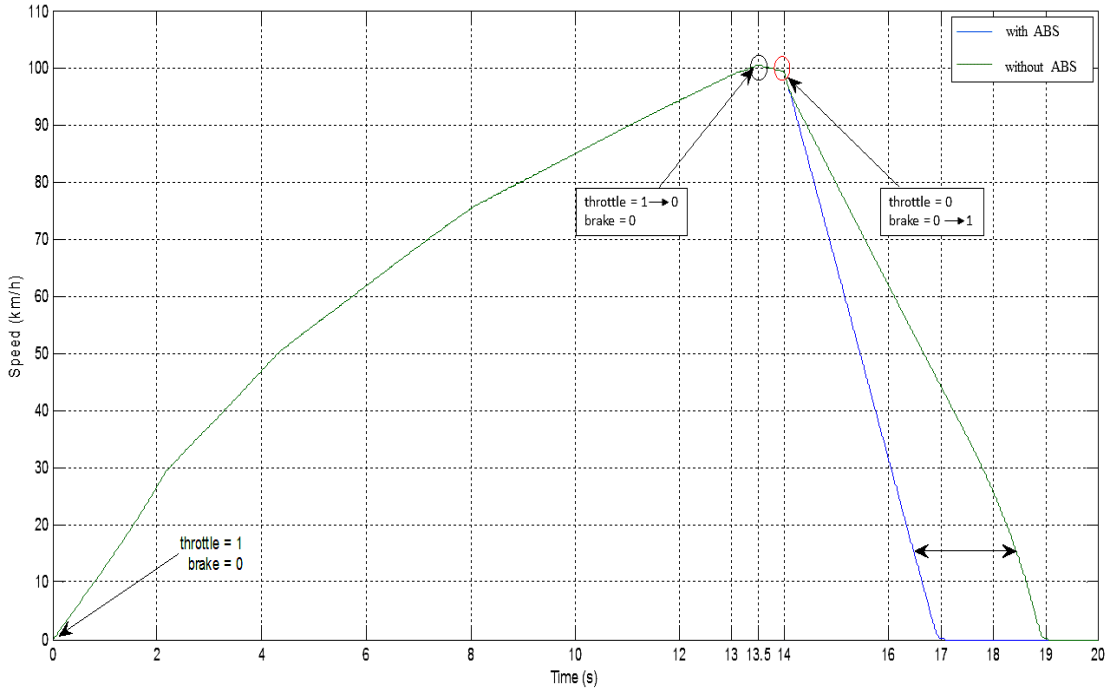

Figure 4.2 Vehicle Speed (km/h) vs Time(s) (S40)

The acceleration (0-100km/h) time during simulations was calculated to be 13.5s. As mentioned in Section 3.2.1, a delay time of 0.5s was considered between full throttle to full brake conditions.

Figure 4.2 displays the braking situation with ABS on/off. The ABS intervention causes the stopping duration to reduce by 2 seconds moving it closer to the original specs.

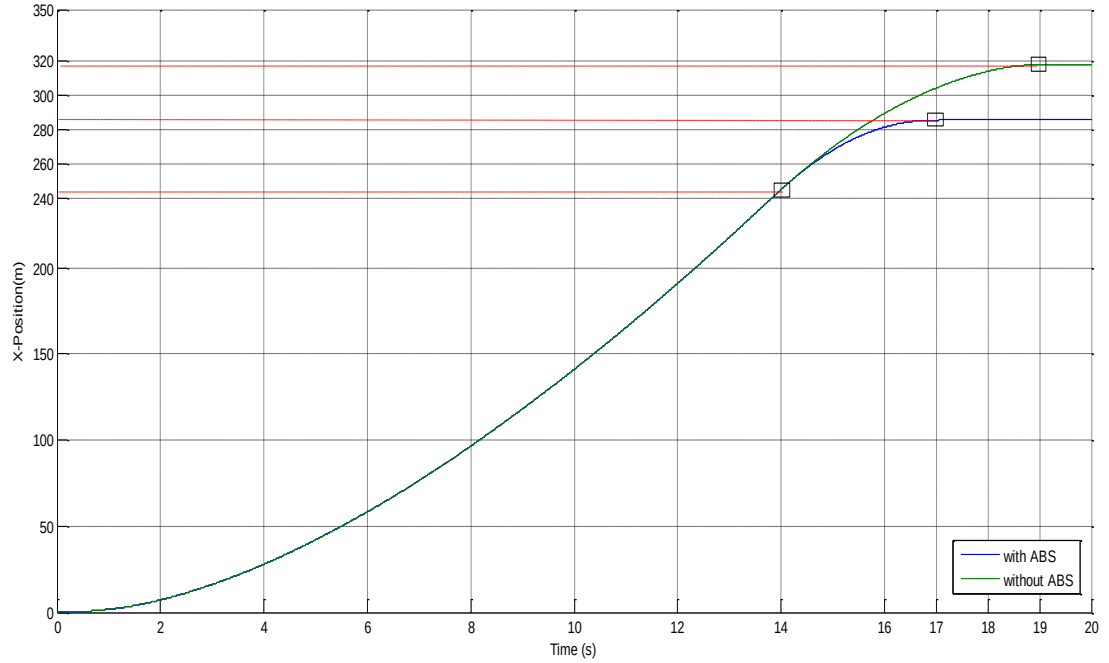

Figure 4.3 X-position (m) vs Time(s) (S40)

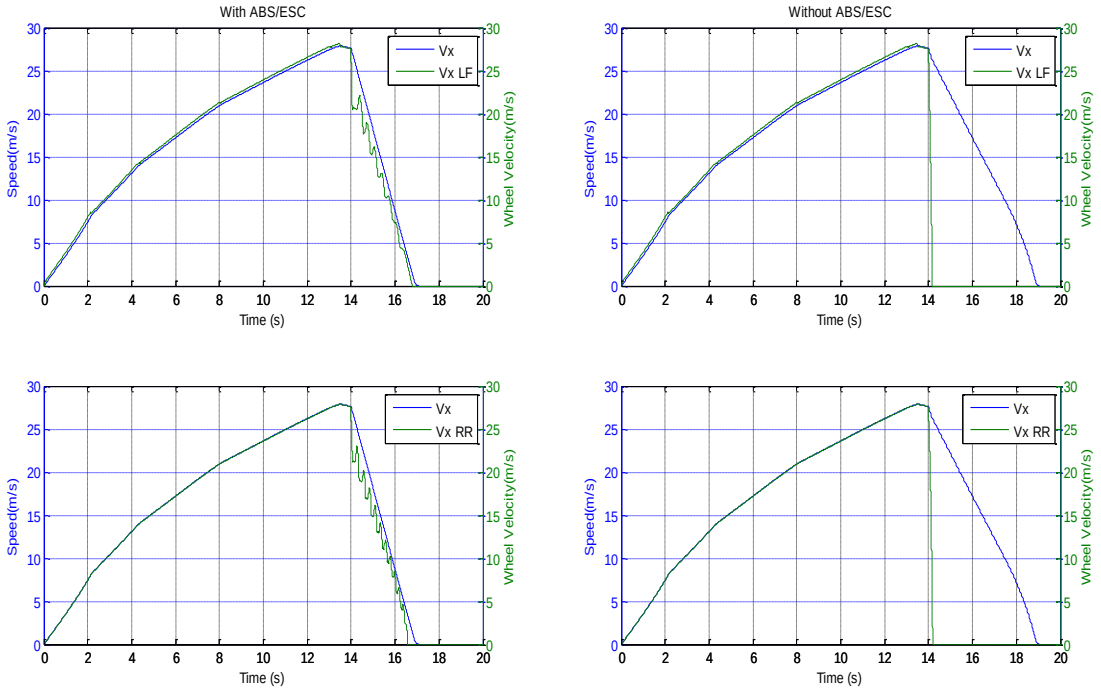

Figure 4.4 Vehicle Velocity (m/s) & Wheel Velocity (m/s) vs Time(s) – LF & RR (S40)

This reduction of 2 seconds causes a difference of 30m in the stopping distance, as shown in Figure 4.3

Figure 4.4 show the velocity comparison between the vehicle and wheel against time. As is the case with a vehicle without ABS, on a full brake condition, the wheel approaches locking condition at increasingly negative longitudinal slip values and hence begins sliding for the duration the vehicle takes to stop. In the case of the S40, for the off condition of ABS, the wheels stops rotating almost within a second of full brake and slide for the remaining duration. This can be seen for all 4 wheels.

Analysis

Table 4.3 Maximum Brake Torque per axle

Vehicle	Axle	Max. Brake Torque (Nm)
Volvo S40	Front	2070
Volvo S40	Rear	1035

With reference to Table 4.1 & 4.4, for the situation when ABS is turned on, the technical and simulation results are similar to one another. However, on comparing the on/off ABS simulation results, the large difference in stopping distances can be attributed to a rigid tire model.

Table 4.4 Simulation Stopping Distance & Duration (S40)

Vehicle	ABS	Stopping Distance - Simulation	Stopping Duration
Volvo S40	Off	70 m	5s
Volvo S40	On	40 m	3s

In the case of active ABS, its influence can be seen clearly in Figure 4.4. With ABS, the brake torque to the wheels is fluctuated with reference to the max brake torque and the range of longitudinal slip around the desired value. Hence, from these results, it can be implied that the ABS is functional and its influence can be tested on the ambulances.

4.2.2 Mercedes Sprinter (2013)

In accordance with the flowchart shown in Figure 3.1, as the ABS was deemed functional, the simulations were carried out for the rear wheel drive Mercedes Sprinter. Before moving to online simulations, parameter tuning for the ABS was carried out after repeated offline tests. A comparison of longitudinal behaviour between offline and online behaviour was carried out.

Table 4.5 ABS Simulation Settings (Sprinter)

ABS Settings	Values
Desired Slip	-0.15
Backlash (Deadband width)	0.05
Controller Gain (I)	2
Controller Gain (P)	10

Table 4.5 displays the ABS settings used for both offline and online simulations for the Mercedes Sprinter. The typical cycle frequency for ABS control is close to 10Hz and this was considered a benchmark for parameter tuning.

The general specification mentioned in Table 4.1 was considered as benchmark for braking tests with the Mercedes Sprinter.

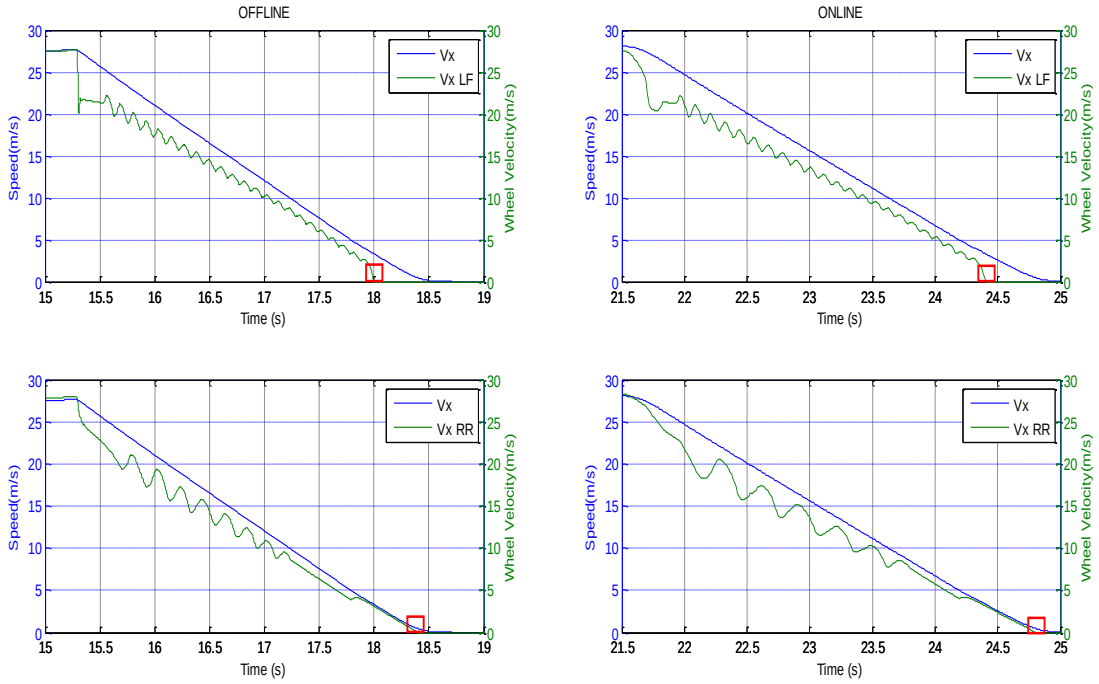

Figure 4.5 Vehicle Velocity (m/s) & Wheel Velocity (m/s) vs Time(s) – LF & RR (with ABS)

With reference to Figure 4.5, the velocity comparison was made for the Left Front and Right Rear tires. For both the cases, it appeared that the front wheels stopped rotating 0.5sec before the rear wheels.

An initial dip in the wheel velocity for the front wheels, not so visible in the rear, at full brake condition, can be attributed to the difference in brake setups between the front and the rear axles especially with respect to the brake pressure gradient.

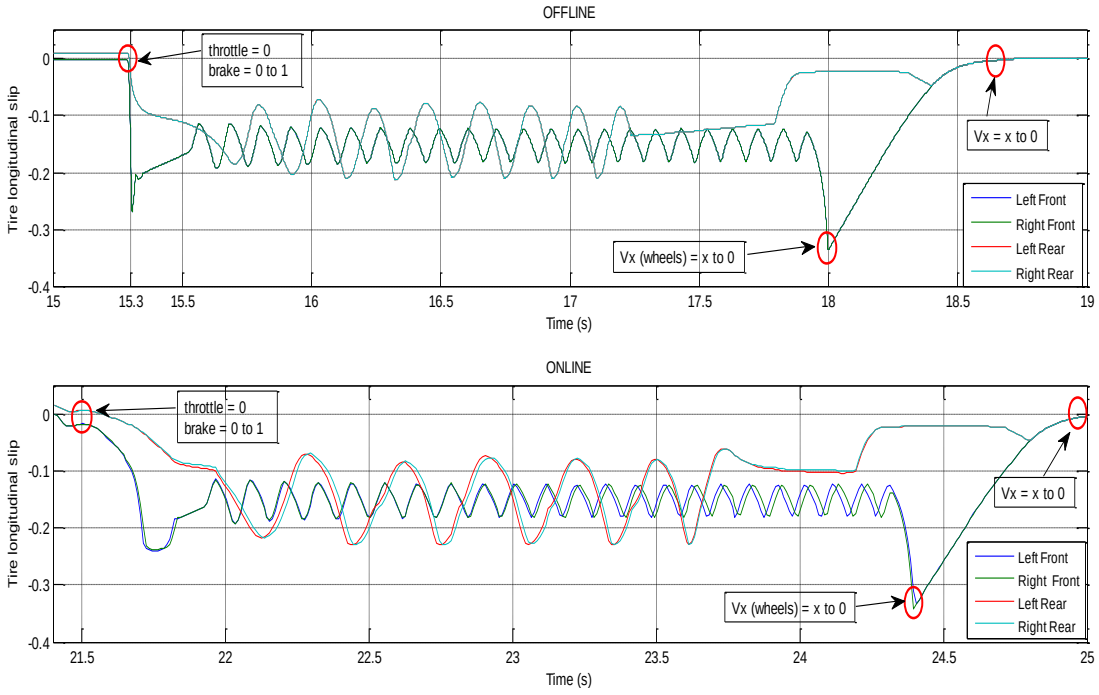

Figure 4.6 Tire Longitudinal Slip vs Time(s) (with ABS)

As stated earlier, the typical cycle frequency for ABS control is close to 10Hz, similar for all 4 wheels. However, in Figure 4.6, for both the offline and online cases, the cycle frequency is different for the front and rear axles.

The cycle frequency for the front axle is close to 8-9Hz whereas at the rear, it is approximately 3-4Hz. A further tuning of the ABS controller is needed to achieve realistic values.

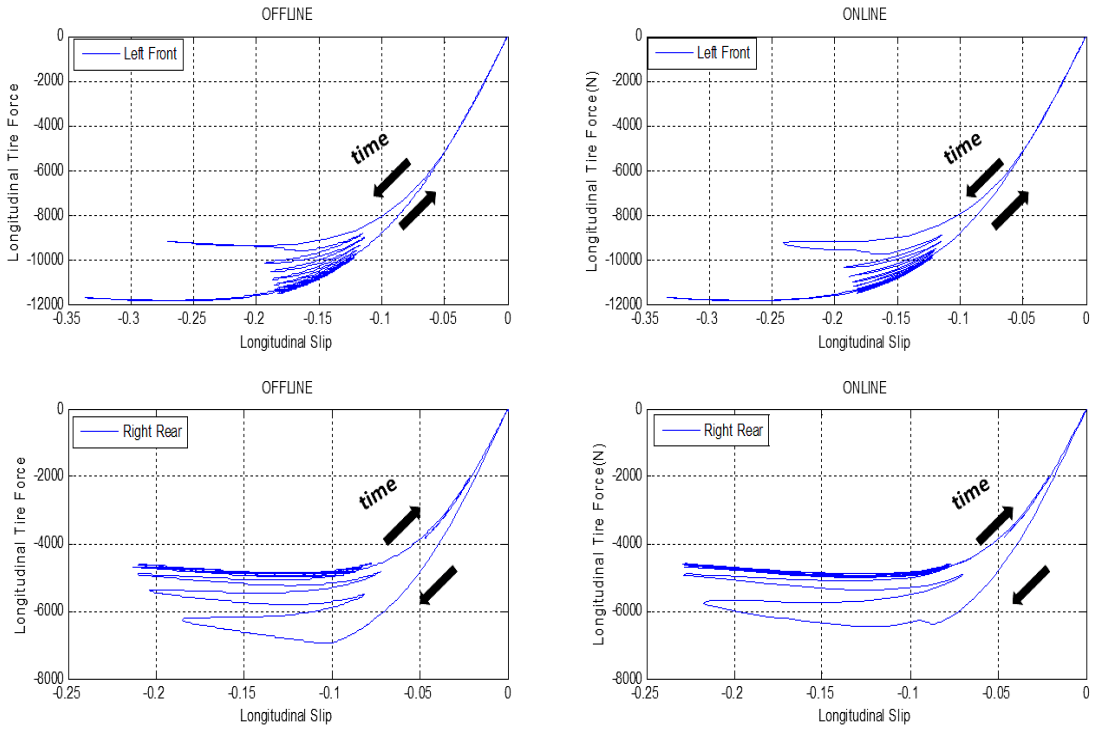

Figure 4.7 Longitudinal Tire Force (N) vs Longitudinal Slip – LF & RR (with ABS)

With reference to Figure 4.1 showing a plot of the longitudinal force coefficient (μ_x) vs longitudinal slip (κ), from the view point of handling, if the wheels were to lock, locking of the rear wheels must be avoided as it triggers directional instability i.e.,

$$\mu_{x2} < \mu_{x1} \tag{4.7}$$

Where,

μ_{x1} = Longitudinal slip coefficient for front wheels (LF, RF)

μ_{x2} = Longitudinal slip coefficient for rear wheels (LR, RR)

In the case of the ambulances, the longitudinal slip is higher at the rear which implies that the rear wheels brake more than required and the braking capacity of the front wheels is under exploited[4]. This can be attributed to unavailability of actual brake system dimensions to compute accurate brake torques. However, this may be achieved by further tuning.

Table 4.6 Maximum Brake Torque per axle

Vehicle	Axle	Max. Brake Torque (Nm)
Mercedes Sprinter	Front	4300
Mercedes Sprinter	Rear	2150

Analysis

Table 4.7 Simulation Stopping Distance & Duration – Sprinter

Vehicle	ABS	Stopping Distance – Simulation	Stopping Duration
Mercedes Sprinter	Off	58 m	4.3 s
Mercedes Sprinter	On	42 m	3.3 s
Mercedes Sprinter (Online)	On	50 m	3.7 s

With reference to Table 4.6 & 4.7 and comparison with Table 4.1, besides the influence of ABS, it is evident that there is a big difference in the results obtained between offline and online simulations. Contributing factors to this difference are attributed, not only to the rigid tire model but also to human delay.

In the case of the offline simulations, the delay mentioned of in Section 3.2.1 is to do with the estimated time taken by the 'driver' to switch between the two pedals (throttle & brake). However, the time taken from brake pedal position = 0 to 100 is not taken into account. But in the case of online simulations, this factor along with HW delay (pedal sensors) causes the difference in the simulation results.

It is evident that the ABS model requires more tuning to achieve closer results but, with reference to research question 2(b) & 3 in Section 1.1.2, the ABS model does survive parameterisation and is reasonably active in the online mode.

4.3 Sine with Dwell Test - Offline

With reference to Section 3.2.3, the SWD tests were performed with different amplitudes. However after studying the data from Test 1 (Steering Amplitude 90 degrees), the intervention from the ESC system is not very distinguishable hence the results from Test 2 are discussed in the subsequent sections. Also, it was necessary to add tuning factor to the model as the braking interventions weren't in the correct range for ESC interventions.

SWD Plots for the base vehicle Volvo S40 are added as Appendix B.

Table 4.8 ESC settings for Mercedes VitoXL

ESC Settings	Values
Cornering Stiffness (Front Axle)	60000 N/rad
Cornering Stiffness (Rear Axle)	90000 N/rad
Velocity Threshold	10 km/h
Yaw Rate Threshold	5 deg/s
Controller Gain (P)	5000
Controller Gain (D)	0

The above settings have been chosen after multiple simulations with witness the most 'visible' ESC intervention.

4.3.1 **Mercedes VitoXL (2013)**

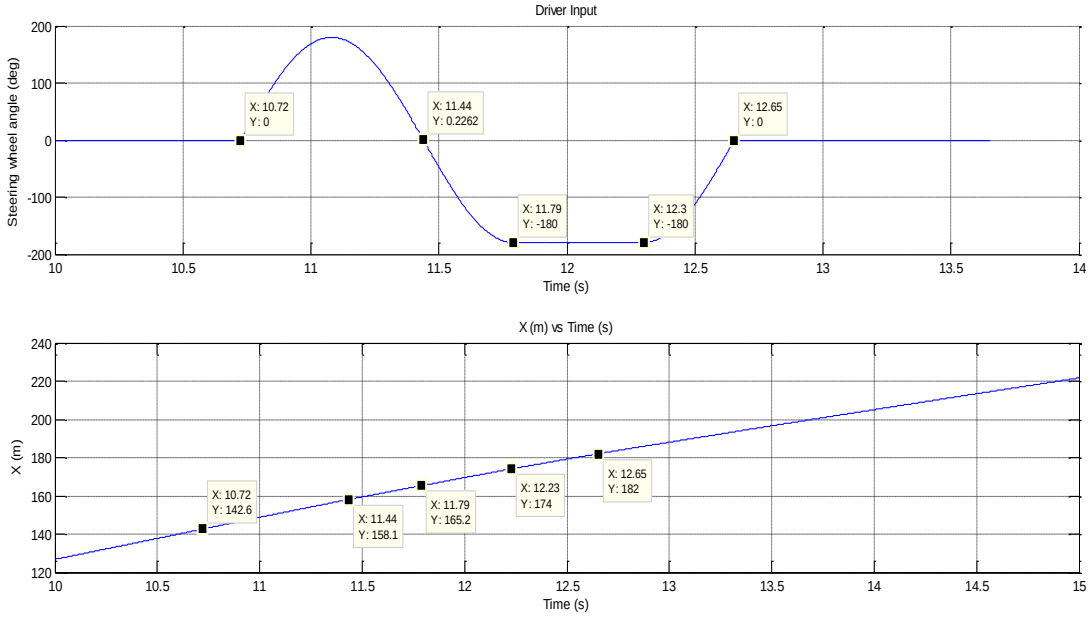

Figure 4.8 Steering Input & Path Plots – Volvo S40 with ESC

With reference to Figure 4.8, the combination of 2 plots provides an indication of the time taken and position coordinates of the vehicle with respect to the steering manoeuvre. A set of 5 points (Table 4.8) have been chosen on the steering angle vs time plot to distinguish the path points and witness the ESC interventions.

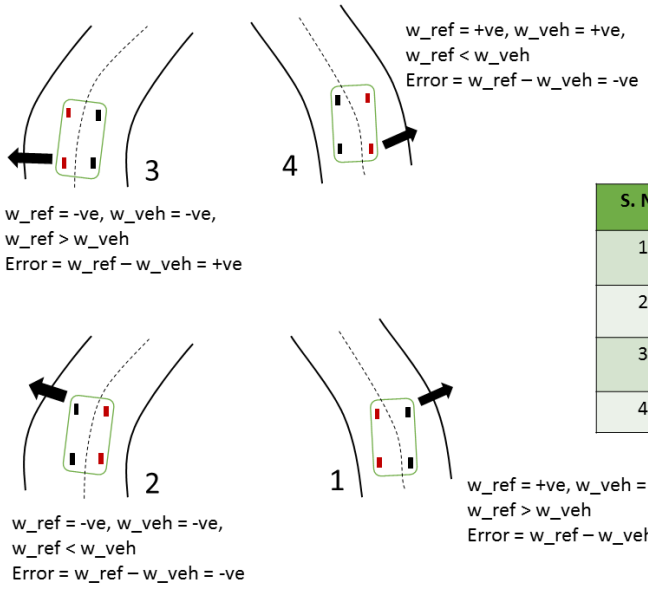

S. No	Vehicle Behaviour	Wheels Braked
1	Understeer	LF & LR
2	Understeer	RF & RR
3	Oversteer	LF & LR
4	Oversteer	RF & RR

Figure 4.9 Vehicle Behaviour for different paths

To break down the possible ESC interventions, Figure 4.9 was constructed. For the SWD manoeuver, the positions 1, 2 and 3 are relevant. As emphasis is based on the oversteer interventions by the ESC, oversteer during the manoeuver is expected in later stages.

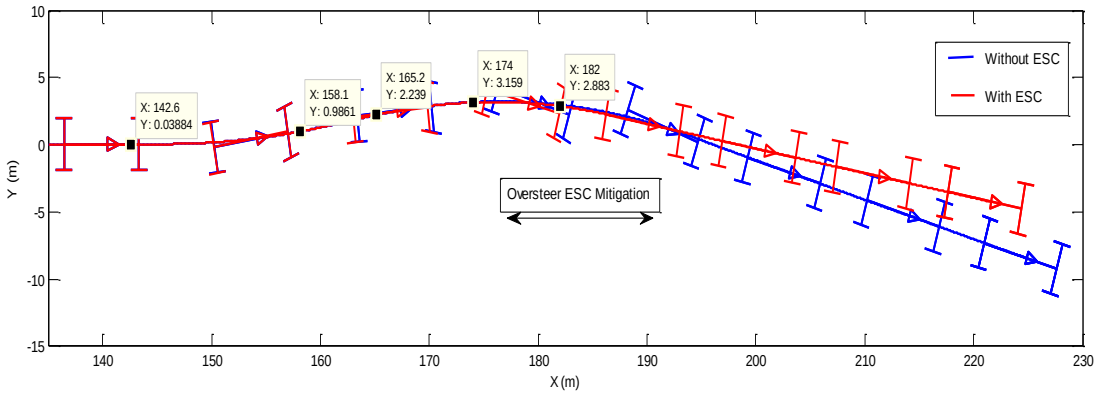

Figure 4.10 Path Plot – Mercedes VitoXL with/without ESC

A path plot (Figure 4.10) was constructed for the manoeuvre with/without ESC enabled. For the simulation with ESC enabled, the brake torque values are shown in Table 4.11. A considerable difference in the final paths is visible after oversteer intervention takes place.

Table 4.9 Steer and Path Points for SWD steer – Mercedes VitoXL with ESC

Steer Point Time (s)	X (m)	Y(m)
10.72	142.6	0.038
11.44	158.1	0.986
11.79	165.2	2.239
12.23	174	3.159
12.65	182	2.888

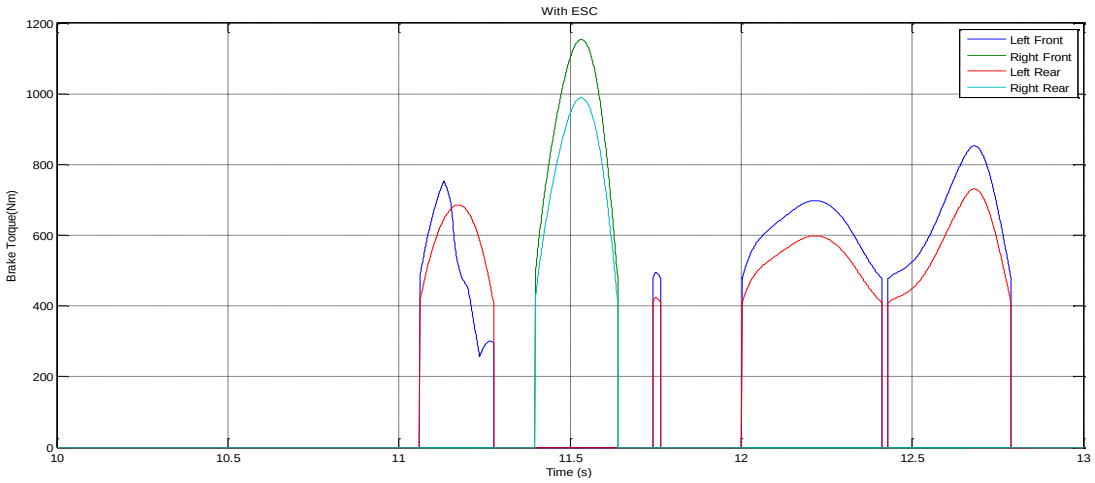

Figure 4.11 Brake Torque (Nm) vs Time (s) – Mercedes VitoXL with ESC

As shown in Figure 4.11, the ESC interventions occur at different time stamps during the entire manoeuver. By referring to Table 4.8, Figure 4.8 & Figure 4.10, it is easy to distinguish when the ESC intervenes and how the vehicle path alters due to these interventions. As emphasis is laid on oversteer intervention, the time interval between 12 – 12.8s is studied.

The stoppage of brake torque for an interval between 12.35 & 12.45s is considered an anomaly as the ESC intervention must mitigate consistently. One of the reasons for this behaviour could be that the plots for reference and actual velocity follow the same trajectory during that short interval, which means ESC does not initialize.

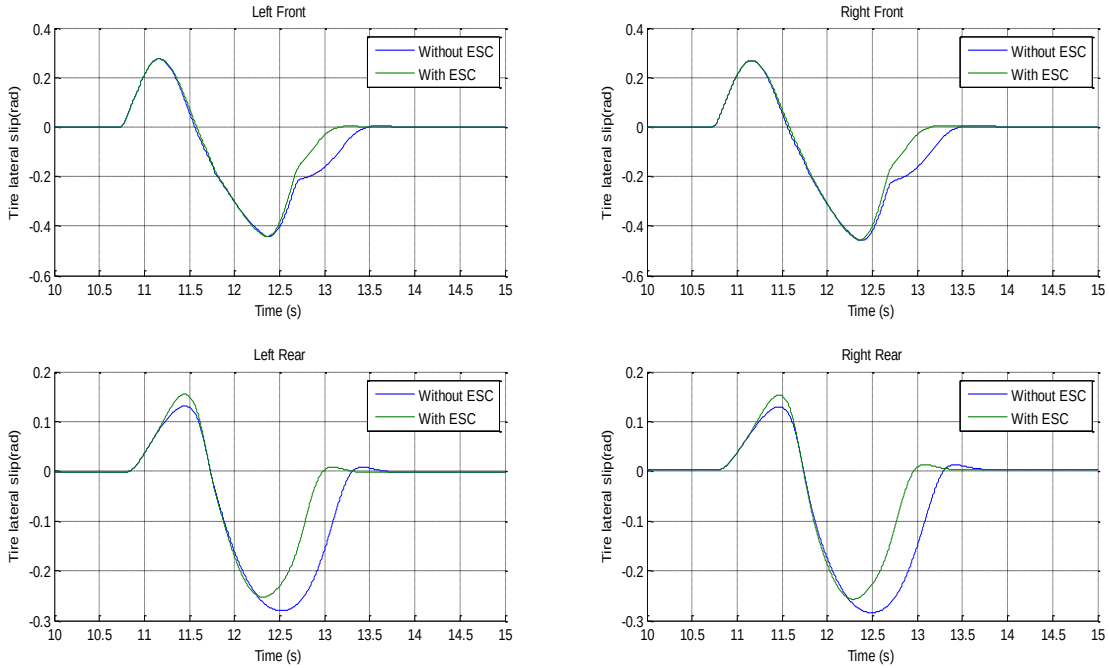

Figure 4.12 Lateral slip angle (rad) vs Time (s) – LF, RF, LR, RR Tires

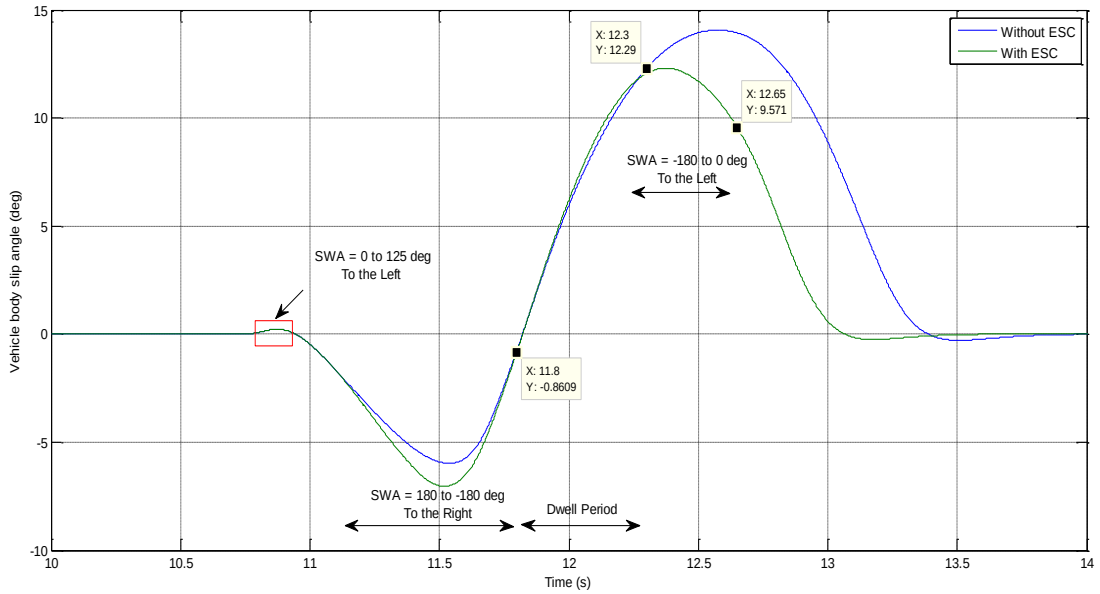

Figure 4.13 Vehicle body slip angle (deg) vs Time (s) – with/without ESC

During that interval, according to the steering manoeuver, the vehicle exits the 'dwell' zone. According to Figure 4.9, slip is expected at the rear wheels due to which the reference velocity is higher than the actual wheel velocity. Condition 3 is applicable and it is visible in the path plots that the vehicle without ESC oversteers more. Hence, the LF and LR wheels are braked for the interval which leads to path correction and the vehicle achieves a more stable path (Figure 4.10).

With reference to Pacejka[3], at low speeds the vehicle slip is negative for right-hand turns. As the slip angles become sufficiently large, the vehicle slip changes into positive values beyond a certain speed.

Considering the above reference, for a left turn when the slip angles are not sufficiently large, Figure 4.13 shows a positive body slip angle but as the tire slip angles increase, the body slip changes to negative values. As the vehicle manoeuvers to the left at the beginning of the SWD, a small peak is visible in Figure 4.13 in correlation with the above statement.

Also, considering the oversteer mitigation zone, a considerable difference in the tire and body slip angles is witnessed supplementing the path correction and stable behaviour discussed in the previous paragraphs.

Conclusion can be drawn that ESC intervenes during oversteer in the dwell period and reduces the side slip. With reference to research question 2(b) in Section 1.1.2, ESC system survives parameterization and intervenes when expected.

4.4 DLC manoeuvre – Online

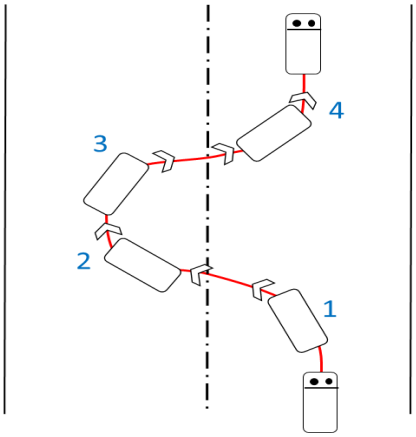

Figure 4.14 DLC path and key positions

Figure 4.14 illustrates the key positions on the DLC track where understeer or oversteer behaviour is expected. Position no 3 (driver turns right, rear axle 'kicks' out) was evaluated as vehicle oversteer zone (see Figure 4.9).

With reference to Section 3.2.3 explaining the dimensions of the DLC track, it is evident that the manoeuvre is complicated and heavily influenced by driver skills[4]. As it is a defined path, subjective evaluation may relay more information than objective measurements. Professional drivers' were not used for this simulation so results may be less indicative of vehicle behaviour than driver skills.

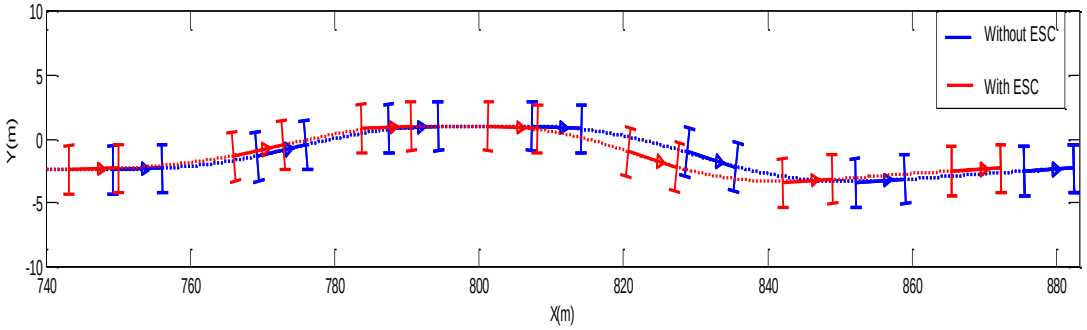

Figure 4.15 DLC path with/without ESC (VitoXL)

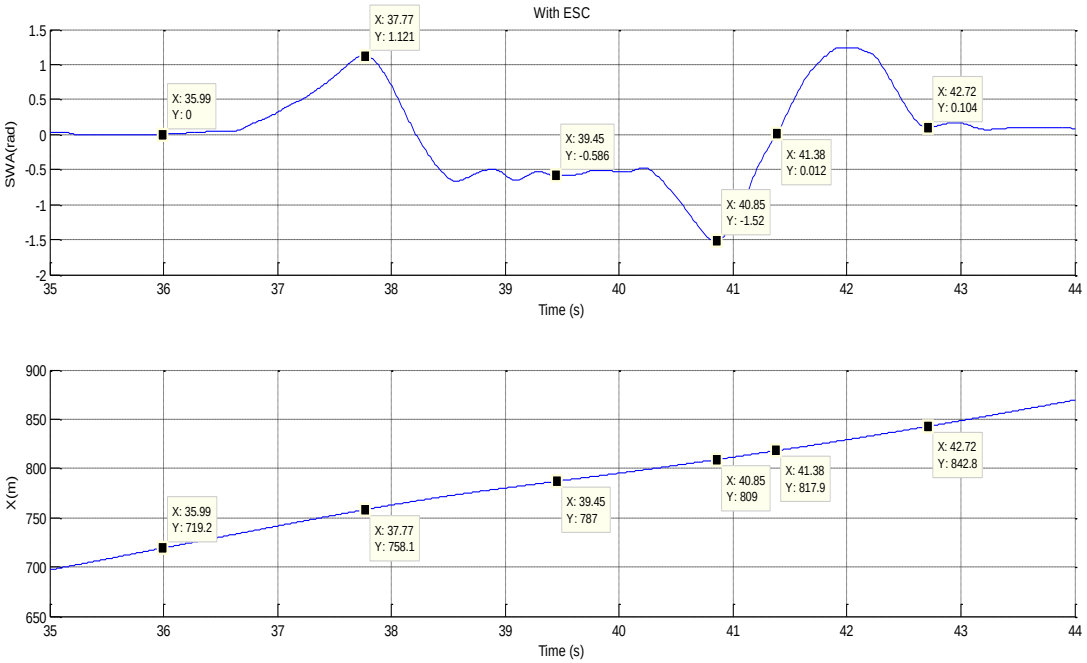

Figure 4.16 Steering Wheel Angle & X-position vs Time (VitoXL)

Figure 4.15 displays the path plotted by a test driver driving the DLC track with/without ESC. With reference to Figure 4.15 and 4.16, it can be estimated that the vehicle path has been altered during the time interval of 41-43 sec which correlates with position 3 in Figure 4.14. However, due to the rigidity of the logging files in the vsim12 project, brake torque is not logged from the system, hence it was impossible to deduce if the ESC intervened during those intervals or not.

The plots displayed in Appendix C show evidence of ESC intervention but it cannot be clearly stated if ESC enabled the test driver to manage a more stable path through the track.

For this reason, plots contemplated during this manoeuvre have not been discussed further.

Analysis

As mentioned in ISO 3888-1[16], repeatability of tests with increasing speeds would provide an outlook about the maximum attainable entry speed without hitting any of the cones. However, when using available drivers, it was impossible to achieve a consistent clean manoeuvre. It was difficult for regular drivers to provide a 'clean' lap without knocking over the cones. Even when the entry velocity was reduced, one or the other cones would always get knocked over as the lack of perception of vehicle width, visually, made it impossible for the driver to 'get his bearings' while driving and adjust his path accordingly.

Lastly, as the input (steering) is not directly comparable (two different runs), it is impossible to maintain consistency.

With reference to research questions 2(b) in Section 1.1.5, it cannot be perceived, in the present state, that the ESC survived parameterization in the online mode.

With respect to research question 3 in Section 1.1.5, the desktop simulator, in its present state, is not considered realistic enough to perceive ESC mitigation.

5 Conclusions & Future Work

5.1 Conclusions

The Chalmers Desktop simulator attempts to bridge the gap between higher fidelity simulators with motion platforms and offline simulations. A fundamental base has been constructed for further development and can be an exciting tool for simulation and scenario testing.

As mentioned earlier, this kind of simulator can be multi-purpose depending on the user. For the ASTAZero project, it is useful as a driver training & risk management tool for ambulance drivers with emphasis on driver behaviour than vehicle behaviour. However, for vehicle model testing, this simulator can be seen as an additional step towards model development and establishing modularity.

In this thesis, a vehicle model is integrated with the software provided by VTI and an attempt is made to explore the modularity of the vehicle model. The vehicle model was parameterized, to a certain extent, to the ambulance vehicles and the general driver feedback was good. A method of scaling with respect to base vehicle (Volvo S40) was adapted to parameterize certain parameters requested by the vehicle model. The parameterisation was verified versus simple specification data, but not against detailed test data.

ABS and ESC systems were integrated into the vehicle model with limited tuning which make them functional but not optimal. Simulation results verify the functions of the ABS and ESC systems but could not validated from track test data.

Regarding the research questions (Section 1.1.5) this thesis has tackled, conclusion can be drawn that the ABS & ESC systems display functionality when fed into the model and simulator. ABS activates during online simulations but ESC intervention couldn't be perceived (research question 1).

Scaling of vehicle parameters with a few parameters was successfully carried out and reasonable vehicle behaviour could be extracted (research question 2(a)). However, being an interesting solution to lack of actual parameters, it may not be ideal.

ABS and ESC systems survived parameterization in the offline mode as they both intervened when necessary but for the online mode, only ABS can be considered active (research question 2(b)).

In the overall sense of a driver simulator, this thesis can state that the simulator is realistic enough to comprehend difference with/without ABS but not realistic enough for ESC activation.

Finally, care must be taken while developing this simulator in the future as it is not intended to be realistic but flexible. Certain solutions may increase realism but care must be taken such that it doesn't lose flexibility. Additions like manual transmission, cruise control system, etc. can be seen as potential improvements.

5.2 Future Work

1. Design traction control, EBD, Torque Converter & Power steering systems
2. ABS & ESC functioning for different friction surfaces.
3. Graphical Interface needed to limit access to VTI SW.
4. Pitch and roll motions to be implemented in driver display to increase level of realism.
5. Implement front hood as visual in desktop simulator for better perception of vehicles boundaries.
6. Remove the dependence on xPC target for real time communication, irrespective of how model executable is generated (Simulink Coder, FMU toolbox, etc).
7. Establish a coordinate translator between vehicle model (in ISO8855) and environment model.
8. The vehicle model is not as robust as perceived earlier, it tends to crash when steering too vigorously in certain situations.

Note – Some deliverables (3, 4, and 6) may have been achieved. Refer to future ASTAZero SIM documentation[8]

6 References

[1] Santoro M. (2014): *Development of a Parameterized Passenger Vehicle Model for Longitudinal Dynamics for a Desktop Driving Simulator*. Master's Thesis. Department of Signals & Systems, Chalmers University of Technology, 2014:08, Göteborg, Sweden, 2014, 22-37 pp.

[2] Morando A. (2014): *Development and improvement of the Chalmers' driving simulator*. Master's Thesis. Department of Signals & Systems, Chalmers University of Technology, EX006/2014, ISSN 99-2747920-4, Göteborg, Sweden, 2014.

[3] Pacejka H. (2006): *Tyre & Vehicle Dynamics*. Elsevier, Jordan Hill, Oxford. 14-41 pp

[4] Genta. G., and Morello. L (2009): *The Automotive Chassis Volume 2: System Design*. Springer Science+Business Media B.V – 2009. 14-31 pp

[5] Mathworks (2014) : *Simulink Real Time*

[6] TNO Automotive (2008) : *MF-Tyre & MF-Swift 6.1 User Manual 2008,* TNO Automotive, The Netheralands. 23-24 pp

[7] Benito G. & Nilsson H., (2006) : *Vehicle Stability Control for Roadside Departure Incidents by Steering Wheel Torque Superposition.* Master's Thesis. Department of Applied Mechanics & Signals and Systems, Chalmers University of Technology, EX020/2006) Göteborg, Sweden 2006, 30 pp.

[8] [ONLINE]: http://www.astazero.com/the-test-site/about/

[9] Olstam J.J (2005): *A model for simulation and generation of surrounding vehicles in driving simulators*. Department of Science & Technology, Linköpings universitet, LIU-TEK-LIC 2005:58, ISBN 91-85457-51-5, ISSN 0280-7971, Norrköping, Sweden, 2005.

[10] Liu A. & Chang S. (1995): Force Feedback in a Stationary Driving Simulator. *IEEE 0-7803-2559-1/95*, Nissan Cambridge Basic Research, Cambridge, MA 02142, 1995

[11] Nagiri S., Doi S., Matsushima S. & Asano K. (1994): Generating method of steering reaction torque on driving simulator. *SSDI 0389-4304(93)E0010-C, JSAE Review 15(1994) 73-86*, Toyota Central Research and Development Laboratories Inc, Aichi, Japan 480-11, 1994

[12] van Putten BJS. (2008): *Design of an Electronic Stability Program for vehicle simulation software*. Master Traineeship. Department of Mechanical Engineering, Automotive Engineering Science, Eindhoven University of Technology, DCT 2008. 138, Eindhoven, the Netherlands, 2008.

[13] Kinjawadekar T.S. (2009): *Model-based Design of Electronic Stability Control System for Passenger Cars Using CarSim and Matlab-Simulink.* Master's Thesis. Department of Mechanical Engineering, The Ohio State University, USA, 2009.

[14] National Highway Traffic Safety Administration (2011): *Laboratory Test Procedure for FMVSS 126, Electronic Stability Control Systems,* Office of Vehicle Safety Compliance, Mail Code: NVS – 220, Washington DC, 2011

[15] International Organization for Standardization (2012): *Passenger cars – Steady-state circular driving behaviour – Open-loop test methods,* ISO 4138:2012(E), Switzerland, 2012.

[16] Swedish Institute for Standards (1999): *Passenger cars – Test track for a severe lane-change manoeuvre – Part 1: Double lane-change,* SS-ISO 3888:1, Stockholm, Sweden, 1999.

[17] International Organization for Standardization (2011): *Road vehicles – Lateral transient response test methods – Open-loop test methods,* ISO 7401:2011(E), Switzerland, 2011.

[18] Swedish Institute for Standards (2006): *Road vehicles – Vehicle dynamics test methods – Part 1: General conditions for passenger cars,* SS-ISO 15037-1:2006, Stockholm, Sweden, 2006.

[19] Swedish Institute for Standards (2011): *Road vehicles – Vehicle dynamics and road-holding ability - Vocabulary,* SS-ISO 8855:2011, Stockholm, Sweden, 2011.

[20] Abou-Zeid M., Kaysi I. & Al-Naghi H. (2011): Measuring Aggressive Driving Behaviour Using a Driving Simulator: An Exploratory Study. *3rd International Conference on Road Safety and Simulation,* American University of Beirut, Indianapolis, USA, 2011.

[21] Swedish Institute for Standards (2007): *Passenger cars – Stopping Distance at straight line braking with ABS – Open-loop test method,* SS-ISO 21994:2007, Stockholm, Sweden, 2007.

[22] Lükert P., Busenthür D., Arndt S. & Sass H. (2013): The Mercedes-Benz OM 651 Four Cylinder Diesel Engine for Worldwide Use. *22nd Aachen Colloquium Automobile and Engine Technology*, Daimler AG, Stuttgart, Germany, 2013.

[23] International Organization for Standardization (2011): *Road Vehicles – Vehicle Dynamics and road-holding ability - Vocabulary,* ISO 8855:2011, IDT, Switzerland, 2011.

Appendix A – Vehicle Model I/O

Sender	Receiver	Bus Name	Signal Name	Description
vsim 12	VDM		watchdog	Linux watchdog counter
vsim 12	VDM		resetIn	Signal to reset the model to original state
vsim 12	VDM		Fxyz_ext_cg	External Forces at centre of gravity (Fx, Fy,Fz) (N)
vsim 12	VDM		Mxyz_ext_cg	External torque at centre of gravity (Mx,My,Mz) (N-m)
vsim 12	VDM		SWA	Steering wheel angle (rad)
vsim 12	VDM		gear_manual	Gear (1-12), 0 = neutral
vsim 12	VDM		clutch_pedal	(0-1)
vsim 12	VDM		throttle	(0-1)
vsim 12	VDM		brake_pedal	Pressure 0-inf or pos 0-100
vsim 12	VDM		P_brk_whls	Brake Pressure [LF,RF,LR,RR] (Pa)
vsim 12	VDM		z_dzdx_dzdy	4 wheels*[z,dzdx,dzdy] (m)
vsim 12	VDM		mu	Friction coeff. For 4 wheels
vsim12	VDM		Vx_max	Max. Longitudinal Velocity (m/s)
vsim12	VDM		auto_gear	Automatic Gear Flag
VDM	vsim 12		xPC watchdog	
VDM	vsim 12		watchdog	Linux watchdog counter
VDM	vsim 12		IDNR	ID number
VDM / Driveline	vsim 12		w_eng	Engine Speed (rad/s)
VDM / Driveline	vsim 12		Tq_eng	Engine Torque (N-m)
VDM / Steer	vsim 12		Tq_SW	Steering Wheel Torque (N-m)
VDM / Chassis	vsim 12	simrefFront Sensor	Vx	Longitudinal Velocity at C.G. (m/s)
VDM / Chassis	vsim 12	simrefFront Sensor	(psi_dot*lf) + Vy	Lateral Velocity at C.G. (m/s)
VDM / Chassis	vsim 12	simrefFront Sensor	Zcg_dot	Vertical Velocity of C.G. (m/s)
VDM / Chassis	vsim 12	simrefFront Sensor	phi_dot	Roll Velocity at C.G. (rad/s)
VDM / Chassis	vsim 12	simrefFront Sensor	teta_dot	Pitch Velocity at C.G. (rad/s)
VDM / Chassis	vsim 12	simrefFront Sensor	psi_dot	Yaw Velocity at C.G. (rad/s)
VDM / Chassis	vsim 12	simrefFront Sensor	ax	Longitudinal Acceleration at C.G. (m/s)
VDM / Chassis	vsim 12	simrefFront Sensor	(psi_2dot*lf) + ay	Lateral Acceleration at C.G. (m/s)

VDM / Chassis	vsim 12	simrefFront Sensor	Zcg_2dot	Vertical Acceleration of C.G (m/s^2)
VDM / Chassis	vsim 12	simrefFront Sensor	phi_2dot	Roll Acceleration at C.G. (rad/s^2)
VDM / Chassis	vsim 12	simrefFront Sensor	teta_2dot	Pitch Acceleration at C.G. (rad/s^2)
VDM / Chassis	vsim 12	simrefFront Sensor	psi_2dot	Yaw Acceleration at C.G. (rad/s^2)
VDM / Chassis	vsim 12	simrefFront Sensor	phi	Roll Angle (rad)
VDM / Chassis	vsim 12	simrefFront Sensor	teta	Pitch Angle (rad)
VDM / Chassis	vsim 12	simrefFront Sensor	psi	Yaw Angle (rad)
VDM / Wheels	vsim 12	log_vector	Fx_body	Longitudinal Tire Force in Body Coordinate system (LF,RF,LR,RR) (N)
VDM / Wheels	vsim 12	log_vector	Fy_body	Lateral Tire Force in Body Coordinate system (LF,RF,LR,RR) (N)
VDM / Axles	vsim 12	log_vector	Fz	Vertical Force (LF,RF,LR,RR) (N)
VDM / Wheels	vsim 12	log_vector	Mz	Aligning Torque (LF,RF,LR,RR) (N-m)
VDM / Wheels	vsim 12	log_vector	LongSlip	Longitudinal Tire Slip (LF,RF,LR,RR)
VDM / Wheels	vsim 12	log_vector	LatSlip	Lateral Tire Slip (LF,RF,LR,RR) (rad)
VDM / Wheels	vsim 12	log_vector	w_whl	Wheel Velocity (LF,RF,LR,RR) (rad/s)
VDM / Chassis	vsim 12	CGSensor	Vx	Longitudinal Velocity at C.G. (m/s)
VDM / Chassis	vsim 12	CGSensor	Vy	Lateral Velocity at C.G. (m/s)
VDM / Chassis	vsim 12	CGSensor	Zcg_dot	Vertical Velocity of C.G. (m/s)
VDM / Chassis	vsim 12	CGSensor	phi_dot	Roll Velocity at C.G. (rad/s)
VDM / Chassis	vsim 12	CGSensor	teta_dot	Pitch Velocity at C.G. (rad/s)
VDM / Chassis	vsim 12	CGSensor	psi_dot	Yaw Velocity at C.G. (rad/s)
VDM / Chassis	vsim 12	CGSensor	ax	Longitudinal Acceleration at C.G. (m/s)
VDM / Chassis	vsim 12	CGSensor	ay	Lateral Acceleration at C.G. (m/s)
VDM / Chassis	vsim 12	CGSensor	Zcg_2dot	Vertical Acceleration of C.G (m/s^2)
VDM / Chassis	vsim 12	CGSensor	phi_2dot	Roll Acceleration at C.G. (rad/s^2)
VDM / Chassis	vsim 12	CGSensor	teta_2dot	Pitch Acceleration at C.G. (rad/s^2)
VDM / Chassis	vsim 12	CGSensor	psi_2dot	Yaw Acceleration at C.G. (rad/s^2)

VDM / Chassis	vsim 12	CGSensor	phi	Roll Angle (rad)
VDM / Chassis	vsim 12	CGSensor	teta	Pitch Angle (rad)
VDM / Chassis	vsim 12	CGSensor	psi	Yaw Angle (rad)
VDM / Steer	vsim 12		front_wheel_angle	0.5(delta_lf+delta_rf)
VDM / Chassis	vsim 12		Z_cab	[Zcg - {1/4(z_dzdx_dzdy_LF+ z_dzdx_dzdy_RF+z_dzdx_dzdy_ LR+z_dzdx_dzdy_RR)}]

Appendix B – SWD Plots Volvo S40

1. Steering Input & Path Plots with ESC

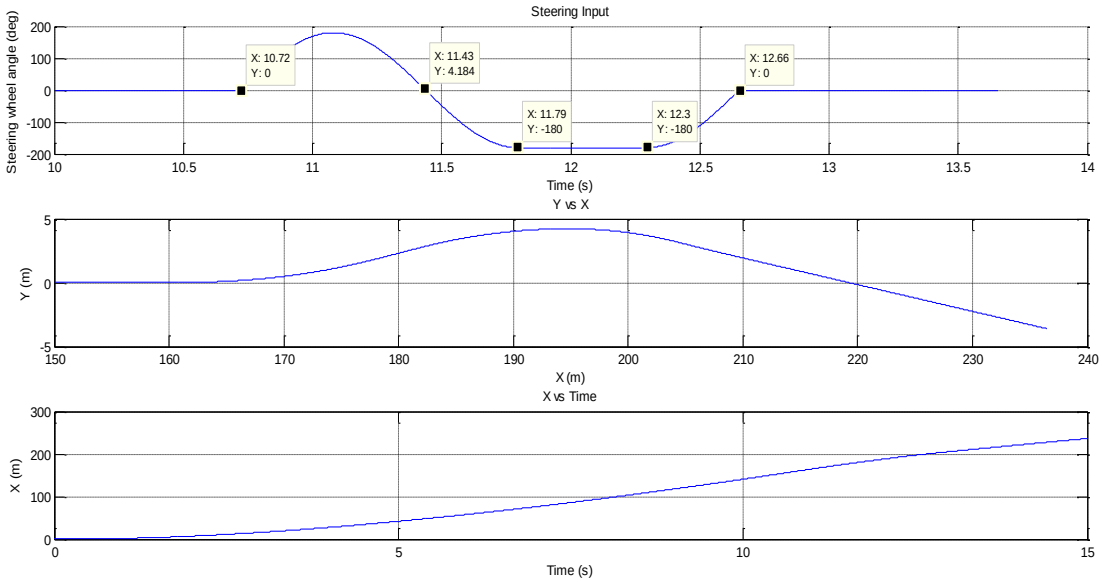

2. Brake Torque (Nm) vs Time (s) with ESC

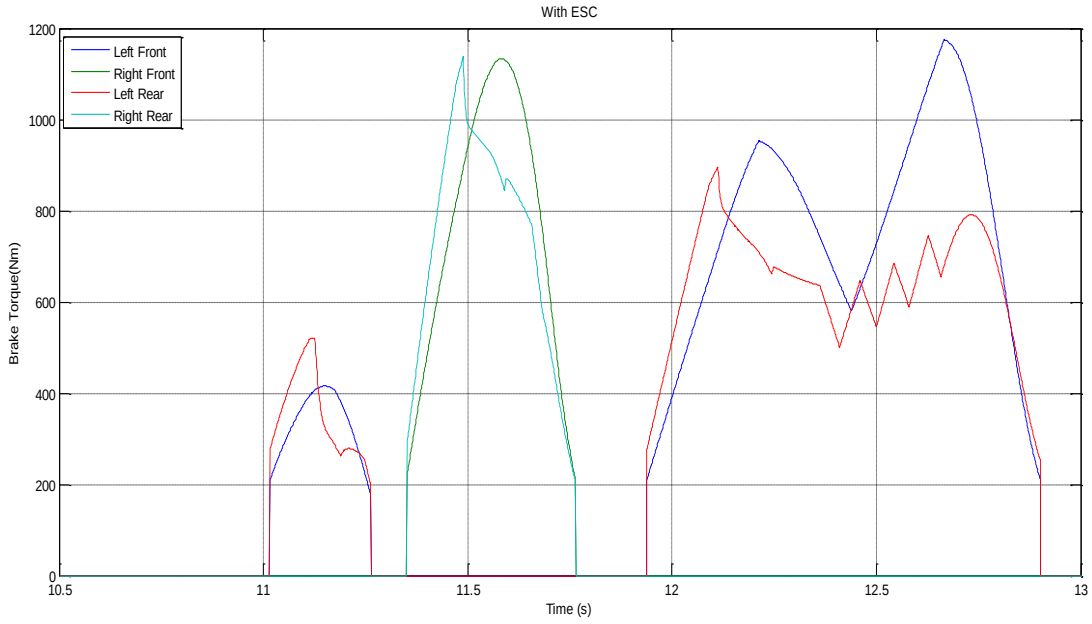

3. Path Plot with/without ESC

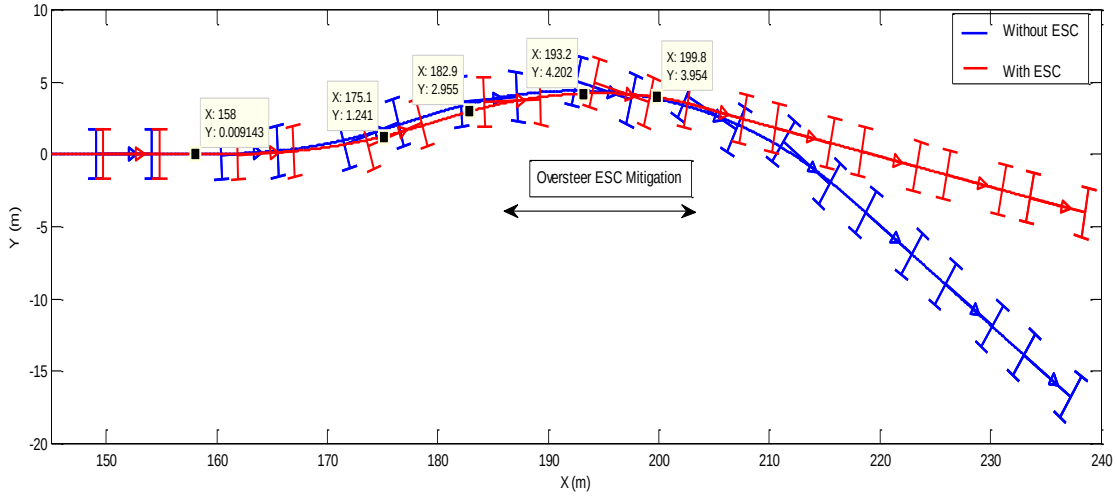

4. Lateral slip angle (rad) vs Time (s) – LF, RF, LR, RR Tires

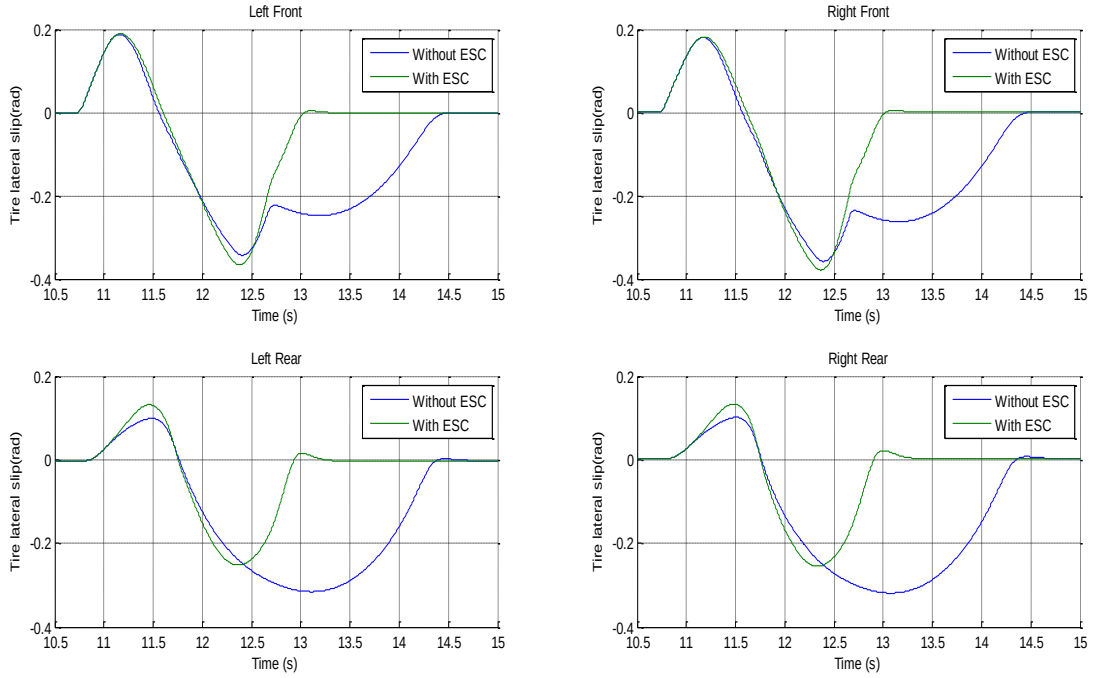

5. Vehicle body slip angle (deg) vs Time (s) – with/without ESC

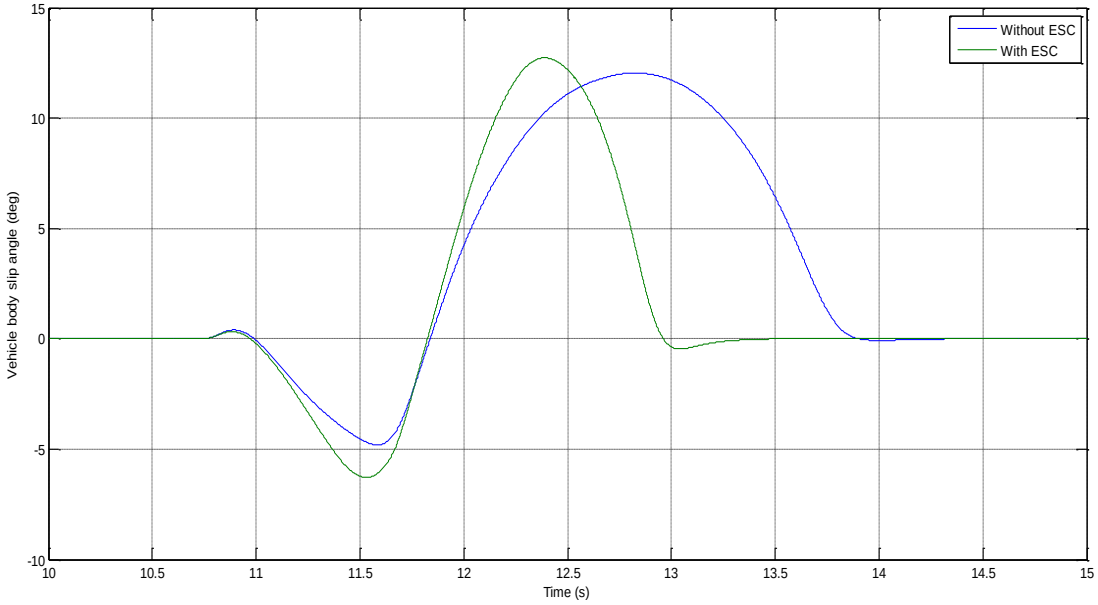

Appendix C – DLC Plots Mercedes VitoXL

1. Lateral Velocity (m/s) & Acceleration (m/s^2) vs Time (s) with/without ESC

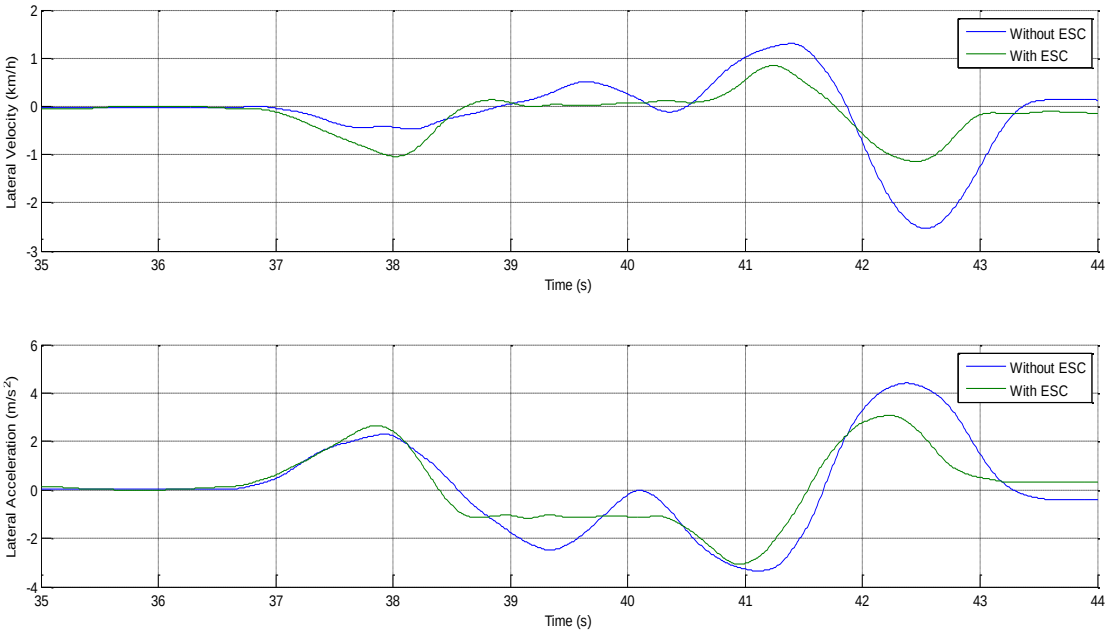

2. Yaw angle (rad) & velocity (rad/s) and Roll angle (rad) & velocity (rad/s) vs Time (s) with/without ESC

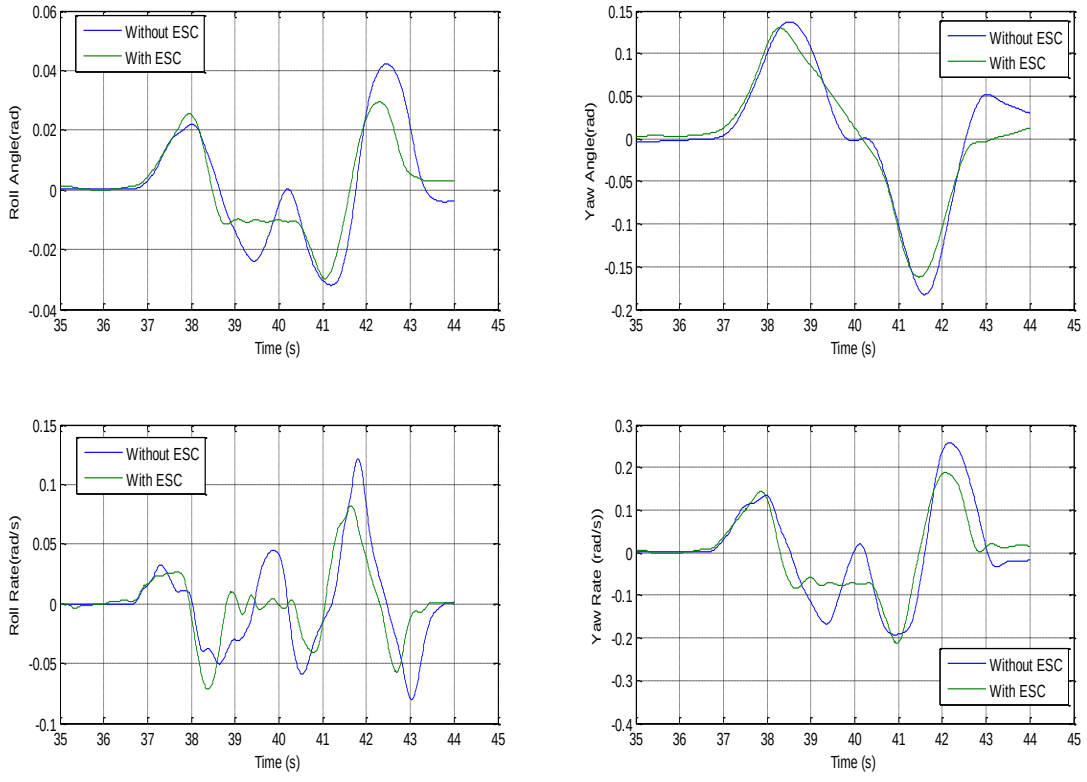

3. Tire Lateral Slip (rad) vs Time (s) with/without ESC – LF, RF, LR, RR

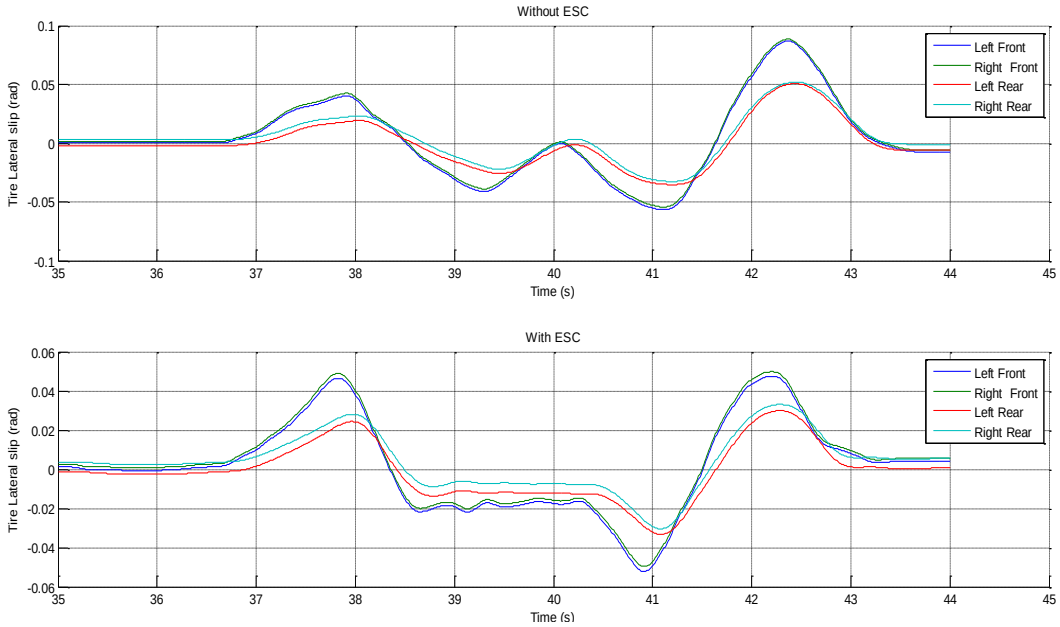

Appendix D - Vocabulary (ISO - 8855)[23]

Reference Frame

Geometric Environment in which all points remain fixed with respect to each other at all times.

Axis System

Set of three orthogonal directions associated with X, Y & Z axes.

Vehicle Axis System

Axis system fixed in the reference frame of the vehicle sprung mass, so that the $X_{vehicle}$ axis is substantially horizontal and forwards (with the vehicle at rest), and is parallel to the vehicle's longitudinal plane of symmetry, and the $Y_{vehicle}$ axis is perpendicular to the vehicle's longitudinal plane of symmetry and points to the left with the $Z_{vehicle}$ axis pointing upward.

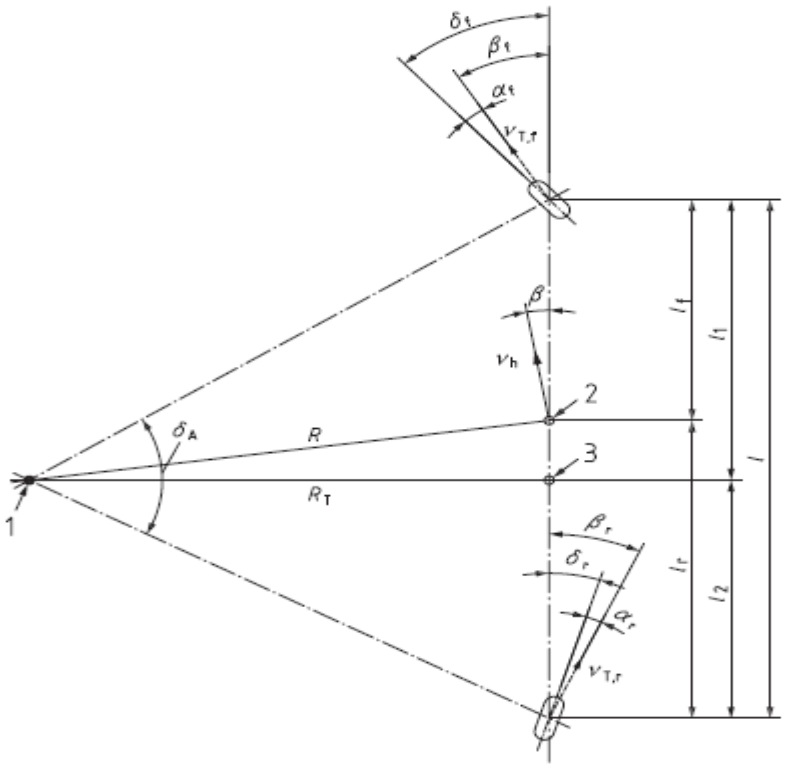

Figure - Slip angles for a single track two-axle model[23]

The following angles are shown positive, vehicle side slip angle, β, front steer angle, δ_f and side slip angle at the front axle, β_f.

The following angles are shown negative, front axle slip angle, α_f, rear steer angle, δ_r, side slip angle at the rear axle, β_f and rear axle slip angle, α_r.

Appendix E – Vehicle Parameters

Vehicle Parameters		Unit	Mercedes Sprinter 319 BlueTec Panel	Mercedes Vito 116 CDI
			Low Roof	Extra Long 4*4
Maximum Speed	Vx_max	[m/s]	161/3.6	174/3.6
Coefficient of Friction(road)	mu	[]	0.750	0.750
Aerodynamic Data				
Projected Frontal Area	A0	[m2]	4.400	4.4
Air Density	rho	[kg/m2]	1.225	1.225
Drag Coefficient	Cax	[]	0.370	0.37
Mass, Inertia, Dimension				
Vehicle Mass	m	[kg]	3500	2800
Unsprung Mass,Front	mus_f	[kg]	226.247	181
Unsprung Mass,Rear	mus_r	[kg]	188.792	151.03
Moment of Inertia about Z axis	Iz	[kgm2]	6007.954	4806.36
Pitch moment of inertia around C.G	Iy	[kgm2]	5061.461	4049.16
Moment of Inertia around roll axis	Ix	[kgm2]	1619.667	1295.73
Centre of Gravity height	h_CG	[m]	0.679	0.679
Unsprung Mass CG height	hus_f	[m]	0.774	0.619
Unsprung Mass CG height	hus_r	[m]	0.774	0.619
Wheel base	wb	[m]	3.665	3.43
Front Axle distance from CG	lf	[m]	1.523	1.425
Track width Front	tw_f	[m]	1.710	1.63
Track width Rear	tw_r	[m]	1.716	1.63

Wheel				
Wheel radius	Rw	[m]	0.300	0.3
Wheel rotational moment of Inertia	Iw	[kgm2]	0.820	0.82
Tire Stiffness	Ktire	[N/m]	379609.544	303687.6356
Tire Damping	Ctire	[N/m]	506.146	404.9168474
Tire Lateral Stiffness	Ky_tire	[N/m]	202458.424	161966.739
Rolling Resistance Coefficient	fr	[]	0.009	0.0094
Tire Relaxation length	Sigma	[]		
Toe, Camber				
Toe-in, Front	toe_f	[rad]	0.001	0.000872665
Toe-in, Rear	toe_r	[rad]	0.003	0.002617994
Static Camber Angle, Front right	gama0_f	[rad]	-0.004	-0.004014257
Static Camber Angle, Rear Right	gama0_r	[rad]	-0.017	-0.017104227
Roll Camber Coefficient, Front	C_gama_phi_f	[]	0.788	0.788
Roll Camber Coefficient, Rear	C_gama_phi_r	[]	0.718	0.718
Coefficient for camber due to lateral force, Front	C_gama_Fy_f	[rad/N]	0.000	4.76475E-06
Coefficient for camber due to lateral force, Rear	C_gama_Fy_r	[rad/N]	0.000	8.02851E-06
Suspension				
Spring Coefficient at wheel position, per side, Front	Kspr_f	[N/m]	50614.606	40491.68474
Damping Coefficient at wheel position, per side, Front	Cdamp_f	[Ns/m]	11388.286	9110.629067

Anti-Roll bar stiffness, Front	Karb_f	[Nm/rad]	85098.337	68078.67
Spring Coefficient at wheel position, per side, Rear	Kspr_r	[N/m]	60737.527	48590.02
Damping Coefficient at wheel position, per side, Rear	Cdamp_r	[Ns/m]	7592.191	6073.75
Anti Roll bar stiffness, Rear	Karb_r	[Nm/rad]	13746.927	10997.54
Roll axle height, Front	hr_f	[m]	0.087	0.086
Roll axle height, Rear	hr_r	[m]	0.097	0.097
Steering system				
Steering Gear Ratio	SG_ratio	[]	23.571	22.06
King pin inclination	teta_kp	[rad]	0.239	0.238
King pin offset (roll steer radius)	d_kp	[m]	-0.0007	-0.0007
Caster Angle	teta_cst	[rad]	0.045	0.045
Caster offset	d_cst	[m]	0.006	0.006
Suspension Compliance for Lateral Force, Front	C_delta_Fy_f	[rad/N]	-1.73835E-06	-1.73835E-06
Suspension compliance for Lateral Force, Rear	C_delta_Fy_r	[rad/N]	3.83972E-07	3.83972E-07
Suspension Torsional Compliance, Rear,	C_delta_Mz_r	[rad/Nm]	0.000023	0.000023
Roll steer coefficient, Front	C_delta_phi_f	[rad/rad]	-0.107	-0.107
Roll steer coefficient, Rear	C_delta_phi_r	[rad/rad]	-0.013	-0.0125
Servo Steering system				
Torsion bar stiffness	Ktb	[Nm/rad]	141.570	132.492
Piston Area	Ap	[m2]	0.001	0.000804

Rack Ratio = rack linear motion per turn of steering wheel	nr	[m/turn]	0.050	0.05
Steering wheel torque below which there will be no servo pressure	T0	[Nm]	1.000	1
Maximum Pressure	Pmax	[bar]	90.000	90
Brake				
Brake torque-line press.grad.Left Front	C_brk_lf	[Nm/Pa]	0.00021	0.000207
Brake torque-line press.grad.Right Front	C_brk_rf	[Nm/Pa]	0.00021	0.000207
Brake torque-line press.grad.Left Rear	C_brk_lr	[Nm/Pa]	0.00021	0.0000495
Brake torque-line press.grad.Right Rear	C_brk_rr	[Nm/Pa]	0.00021	0.0000495
Driveline				
Drive-shaft moment of inertia per side	Idrv	[kgm2]	1.006	0.94
Engine				
Engine Rotational moment of inertia	Ieng	[kgm2]	0.2	0.2
Engine Throttle	eng_throttle	[%]	[0 2.5 9 12 18 21 25 30 35 40 50 100]	[0 2.5 9 12 18 21 25 30 35 40 50 100]
Engine Speed	eng_speed	[rad/s]	[0 105 130 145 190 235 280 325 370 400 415 440]	[0 105 157 209 262 314 367 419 471 524 681]
Engine Torque	eng_torque	[Nm]	-	-
Engine Idle speed	w_eng_idle	[rad/s]	100	100

Maximum engine speed	w_eng_max	[rad/s]	630	712
Gearbox				
Gear ratios	gear_ratio	[]	[5.076 2.610 1.518 1.0 0.791 0.675]	[3.595 2.186 1.405 1.0 0.831]
Speed for shifting up the gear, automatic gearbox	gear_up_Vx	[m/s]	[1.25 9.0 17.0 21.5 25.5]	[7.0 13.0 21.0 26.5]
Speed for shifting down the gear, automatic gearbox	gear_down_Vx	[m/s]	[1 5 14 19.5 24.5]	[6.5 12.5 19.5 25.5]
End gear ratio	endgear_ratio	[]	3.923	3.273

Appendix F – Logged Variables

S.NO	DATA FIELD	DESCRIPTION	UNIT
1	timer	Absolute simulator time since program start	s
2	odometer	Distance driven	m
3	road_id	Current road id	-
4	s	longitudinal position, s in Track system	m
5	r	lateral position, r in Track system	m
6	yaw	Yaw angle relative to road tangent	rad
7	vx	Body fixed longitudinal velocity	m/s
8	vy	Body fixed lateral velocity	m/s
9	ax	Body fixed longitudinal acceleration	m/s2
10	ay	Body fixed lateral acceleration	m/s2
11	yaw_vel	Yaw velocity	rad/s
12	eng_torq	Engine torque	Nm
13	engine_rps	Engine revolution	rad/s
14	throttle	Throttle position, 0 no throttle	-
15	brake_pedal_active	Brake pedal active	-
16	brake_pedal_press	Brake pedal pressure	kPa
17	brake_force	Approx. brake force applied to pedal	N
18	stw_angle	Steering wheel angle, CCW positive	rad
19	stw_torq	Steering wheel torque	Nm
20	left_indicator	Left indicator, 1 = active	-

21	right_indicator	Right indicator, 1 = active	-
22	gear	Gear number	-
23	event_id	Active event's id (see below)	-
24	event_state	Current state in active event	-
25	event_state_timer	Time spent in current state	s
26	X	Global X coordinate	m
27	Y	Global Y coordinate	m
	Data Field	Description	Unit
28	watchdog	Linux watchdog counter	-
29	resetIn	Signal to reset the model to original state	-
30-32	Fxyz_ext_cg	External Forces at centre of gravity	N
33-35	Mxyz_ext_cg	External torque at centre of gravity	Nm
36	SWA	Steering wheel angle	rad
37	gear_manual	Gear (1-12), 0 = neutral	-
38	Clutch	(0-1)	%
39	throttle	(0-1)	%
40	brake_pedal_input	Pressure 0-inf or pos 0-100	%
41-52	z_dzdx_dzdy	4 wheels*[z,dzdx,dzdy]	m
53-56	mu	Friction coeff. For 4 wheels	
57-60	P_brk_wheels	Brake Pressure [LF,RF,LR,RR]	Pa
61	Vx_max	Max. Longitudinal Velocity	m/s
62	auto_gear	Automatic Gear Flag	
63	xPC watchdog		-
64	watchdog	Linux watchdog counter	
65	IDNR	ID Number	-
66	w_eng	Engine Speed	rad/s
67	Tq_eng	Engine Torque	Nm
68	Tq_SW	Steering Wheel Torque	Nm
69	Vx	Vehicle Model longitudinal velocity	m/s
70	(psi_dot*lf) + Vy	Vehicle Model Lateral velocity	m/s
71	Zcg_dot	Vertical Velocity of COG	m/s
72	phi_dot	Roll Velocity at COG	rad/s
73	teta_dot	Pitch Velocity at COG	rad/s
74	psi_dot	Yaw Velocity at COG	rad/s
75	ax	Longitudinal Acceleration	m/s^2
76	(psi_2dot*lf) + ay	Lateral Acceleration	m/s^2
77	Zcg_2dot	Vertical Acceleration of COG	m/s^2
78	phi_2dot	Roll Acceleration at COG	rad/s^2
79	teta_2dot	Pitch Acceleration at COG	rad/s^2
80	psi_2dot	Yaw Acceleration at COG	rad/s^2

81	phi	Roll Angle at COG	rad
82	teta	Pitch Angle at COG	rad
83	psi	Yaw Angle at COG	rad
84-87	Fx_body	Longitudinal Tire Force in body coordiante system[LF,RF,LR,RR]	N
88-91	Fy_body	Lateral Tire Force in body coordinate system [LF,RF,LR,RR]	N
92-95	Fz	Vertical Tire Force [LF,RF,LR,RR]	N
96-99	Mz	Tire Aligning Torque [LF,RF,LR,RR]	Nm
100-103	LongSlip	Tire Longitudinal Slip [LF,RF,LR,RR]	-
104-107	LatSlip	Tire Lateral Slip[LF,RF,LR,RR]	rad
108-111	w_whl	Wheel Velocity	rad/s
112	Zero Vector	-	-
113	Vx	Longitudinal Velocity	m/s
114	Vy	Lateral Velocity	m/s
115	Zcg_dot	Vertical Velocity of COG	m/s
116	phi_dot	Roll Velocity at COG	rad/s
117	teta_dot	Pitch Velocity at COG	rad/s
118	psi_dot	Yaw Velocity at COG	rad/s
119	ax	Longitudinal Acceleration	m/s^2
120	ay	Lateral Acceleration	m/s^2
121	Zcg_2dot	Vertical Acceleration of COG	m/s^2
122	phi_2dot	Roll Acceleration at COG	rad/s^2
123	teta_2dot	Pitch Acceleration at COG	rad/s^2
124	psi_2dot	Yaw Acceleration at COG	rad/s^2
125	phi	Roll Angle at COG	rad
126	teta	Pitch Angle at COG	rad
127	psi	Yaw Angle at COG	rad
128	front_wheel_angle	0.5(delta_lf+delta_rf)	rad
129-138	Z_cab		m